Evidence for a 200 km thick diamond-bearing root beneath the Central Mackenzie Valley, Northwest Territories, Canada? Diamond indicator mineral geochemistry from the Horn Plateau and Trout Lake regions

Stéphane P. Poitras[1] • David G. Pearson[1] • Matthew F. Hardman[1] • Thomas Stachel[1] • Geoff M. Nowell[2] • Scott Cairns[3]

✉ S.P. Poitras
spoitras@ualberta.ca

[1] Department of Earth and Atmospheric Sciences, University of Alberta, 1-26 Earth Sciences Building, Edmonton, AB, T6G 2E3

[2] Department of Earth Sciences, Durham University, Science Labs, Durham, UK, DH1 3LE

[3] Northwest Territories Geological Survey, 5310 44 Street, Yellowknife, NT, X1A 1K3

Abstract The Central Mackenzie Valley (CMV) area of Northwest Territories is underlain by Precambrian basement belonging to the North American Craton. The potential of this area to host kimberlitic diamond deposits is relatively high judging from the seismologically-defined lithospheric thickness, age of basement rocks (2.2-1.7 Ga) and presence of kimberlite indicator minerals (KIMs) in Quaternary sediments. This study presents data for a large collection of KIMs recovered from stream sediments and till samples from two study areas in the CMV, the Horn Plateau and Trout Lake. In the processed samples, peridotitic garnets dominate (> 25 % at each location) while eclogitic garnet is almost absent in both regions (< 1 % each). KIM chemistry for the Horn Plateau indicates significant diamond potential, with a strong similarity to KIM systematics from the Central and Western Slave Craton. The most significant issue to resolve in assessing the local diamond potential is the degree to which KIM chemistry reflects local and/or distal kimberlite bodies. Radiogenic isotope analysis of detrital kimberlite-related CMV oxide grains requires at least two broad age groups for eroded source kimberlites. Statistical analysis of the data suggests that it is probable that some of these KIMs were derived from primary and/or secondary sources within the CMV area, while others may have been transported to the area from the east-northeast by Pleistocene glacial and/or glaciofluvial systems. At this stage, KIM chemistry does not allow the exact location of the kimberlitic source(s) to be constrained.

Key words:

Kimberlite indicator minerals

Garnet

Ilmenite

Hf isotopes

Geothermobarometry

Diamond exploration

Character count: 75,799 Characters (with spaces)

64,599 Characters (no spaces)

Introduction

Since the discovery of the first diamondiferous kimberlite in the Lac de Gras area in 1991, more than 300 kimberlites - many diamondiferous - have been identified in the Northwest Territories (NT). These discoveries have provided new suites of peridotite and eclogite xenoliths, as well as diamonds, generating considerable interest in the mantle beneath the Slave Craton. Despite the economic significance of diamond mines from the Central Slave Craton, relatively little research has been conducted on the remaining portions of cratonic lithospheric mantle underlying other parts of northern Canada, such as the area west of the Slave Craton margin. The possible existence of thick and cold cratonic lithosphere in the Central Mackenzie Valley (CMV), NT, more than 200 kilometres west of the Slave Craton margin (Fig. 1), is currently poorly constrained. This area, south of Great Bear Lake, has seen limited diamond exploration. Olivut Resources Ltd. is currently exploring this area and have reported the discovery of at least 29 kimberlites (two diamondiferous) since the commencement of their HOAM project in 1993 (Fig. 1; Pitman 2014). The reported kimberlite indicator mineral (KIM) chemistry from these kimberlites (Pitman 2014) differs from data obtained during regional stream sediment and till sampling (Day et al. 2007; Mills 2008; Pronk 2008) suggesting the possible presence of additional, potentially diamondiferous sources within the CMV or complex mineral transport into the region.

Although the CMV region is not a traditional Archean "cratonic" setting in terms of its crustal geology - a widely accepted pre-requisite for diamondiferous kimberlites (Janse 1994) - discoveries of primary diamond occurrences in North America have been made in similar settings (e.g., Buffalo Head Hills). Furthermore, the LITHOPROBE Slave-Northern Cordillera Lithospheric Evolution (SNORCLE) transect line 1 (e.g., Cook et al. 1999) and more recent regional-scale surface-wave seismic tomography studies (e.g., Schaeffer and Lebedev 2014) indicate the likely presence of thick (~ 200 km), cold lithospheric mantle extending into the diamond stability field, underpinning an area of several hundreds of square kilometres across the CMV (Fig. 1). In this study, we present new geochemical data for a large collection of KIMs sampled from two regions within the CMV: Horn Plateau (25,233 km^2) northeast of the Mackenzie River and > 175 km west of Yellowknife and Trout Lake (10,680 km^2) south of the Mackenzie River (Figs. 1-2; for river, lake and place locations see Figures S1-S2). KIM chemistry of grains from these regions will be used to assess their diamond potential and improving our understanding of potential kimberlite sources.

Geological Setting

Precambrian Geology

The Precambrian basement of the Wopmay Orogen (ca. 1.95-1.85 Ga; Davis et al. 2015; Ootes et al. 2015) is known from a few oil and gas exploration wells (Burwash et al. 1993 and references therein) plus inferences made from geophysical survey data in the CMV (Cook et al. 1999; Aspler et al. 2003; Cook and Erdmer 2005). From east to west under the Phanerozoic strata is Precambrian basement from the 1.88-1.85 Ma Great Bear Magmatic Zone, the 1.95-1.89 Ga Hottah Terrane, the ca. 1.84 Ga Fort Simpson Terrane (magnetic high) and the cryptic Nahanni magnetic low (Villeneuve et al. 1991; Aspler et al. 2003; Cook and Erdmer 2005). In the extreme northeast of the CMV, Precambrian crystalline and metasedimentary rocks outcrop on the exposed Canadian Shield (Fig. 1). In the eastern Horn Plateau region, Precambrian rocks occur at only 400 m depth (Burwash et al. 1993) and dip gently towards the west-southwest to depths of greater than two kilometres in the westernmost areas (Gal and Lariviere 2004).

Phanerozoic Geology

The CMV lies in the northern portion of the Phanerozoic Western Canadian Sedimentary Basin known as the Northwest Territories Interior Platform. The nearly horizontal, mostly undeformed Phanerozoic sedimentary rocks are disrupted by highs of underlying Precambrian basement from episodes of uplift, erosion and subsidence (Dixon 1999). In the extreme northeast of the CMV, near Lac la Martre, Cambrian to Middle Devonian strata outcrop (Fig. 1). In the northern Horn Plateau, Cambrian rocks overlie the Precambrian basement, except over the Bulmer Lake gravity high (Fig. 1), where they were either eroded and/or not deposited. Elsewhere Cambrian sediments appear to have been largely removed or were not deposited (Meijer Drees 1993). Ordovician and Silurian rocks still exist at depth in the northern part of the Horn Plateau, north of about 62 °N, while south of 62 °N, Middle-Late Devonian strata directly overlies the basement (Fig. 1; Williams 1985; Meijer Drees 1993; Pitman 2014). A prominent series of low escarpments of Devonian limestone located on the southern edge of the Horn Plateau are an exception to the otherwise monotonous, limited outcrop landscape (Craig 1965).

Cretaceous strata are only preserved in the extreme northwest and in higher areas where they have not been removed by erosion in the Horn Plateau region (e.g., Horn Plateau and Ebbutt Hills; Fig. 1) and are covered by glacial till and organics, with few recorded outcrops in the CMV (Craig 1965; Meijer Drees 1993). On the Horn Plateau, flat-lying Albian marine shales and minor sandstones unconformably overlie Late Devonian strata (Craig 1965; Meijer Drees 1993; Dixon 1999) with the Albian strata reaching ~ 60 m thick east of Willow Lake on the plateau and ~ 100 m thick east of Ebbutt Hills (Dixon 1999). South of ~ 61 °N, Late Aptian to Campanian strata (Fort St. John Group) are widespread (Fig. 1). East and southeast of Trout Lake, Cretaceous strata lies unconformably, from north to south, on Devonian and Carboniferous strata (Stott et al 1993) whereas to the southwest this unit is completely absent (Dixon 1999). Cenomanian-Turonian aged marine shales are only preserved in the eastern Trout Lake region, with only Early-Middle Cenomanian regressive sandstone beds (Dunvegan Formation) found capping some hills to the northwest and southeast of Trout Lake (Dixon 1999).

Quaternary Geology

The CMV is almost entirely covered with a mantle of glacial and post-glacial deposits (Figs. 2, S2). Morainal tills blanket most of the CMV and are locally ridged or hummocky, while colluvial deposits and local undifferentiated bare rock outcrops are found along the southern escarpment of the Horn Plateau. To the north and northwest of the Horn Plateau, alluvial gravel and sand occupy flood plains and terraces along streams (Rutter et al. 1993). South of the plateau, organic (fen and bog) deposits overlie a massive till plain (Rutter et al. 1993; Fulton 1995). In the Mackenzie, Liard, Willowlake and other river valleys, fine-grained organic, eolian, glacio- and/or -fluvial and -lacustrine deposits blanket till, older deposits and bedrock below 220 m elevation (Fig. 2). North of the Horn Plateau, glacial deposits are up to 81 m thick (Craigie 1991), while in the Fort Simpson area the maximum thickness is 120 m (Ghaznavi et al. 1986). In the western and eastern parts of the CMV on the Liard and Last Stop mineral claims of Olivut Resources, below glaciofluvial outwash, till is between 10-60 m thick (Pitman 2014). In contrast, thinner unconsolidated Quaternary deposits (10-20 m) typically exist throughout the lowlands and major river valleys in the Horn Plateau, as well as most of the Trout Lake (Rutter et al. 1993; Huntley et al. 2006, 2008).

Highlights of the CMV Quaternary history include intervals of continental glaciation involving complex frontal retreat and ice stagnation, glacial lake formation and meltwater drainage (Huntley et al. 2006, 2008). At the last glacial maximum (ca. 18 ka), the entire CMV was completely covered by the Laurentide Ice Sheet with a thickness > 1000 m, implied by the appearance of granitic erratic boulders at ~ 1500 m elevation to the west of the CMV (Huntley et al. 2008). The advance of this continental ice-sheet resulted in the erosion, transport, dispersal and deposition of bedrock and pre-existing sediment within the CMV. The highlands of Ebutt and Martin Hills and the Horn Plateau are believed to have slightly deflected the regional advance of the ice-sheet (Rutter et al. 1993; Fulton 1995). To date, the only ice-flow features reported on top of the Horn Plateau are small drumlinoid features on the northeast edge of the plateau (Craig 1965), which mark the youngest ice-flow direction trending west-southwest (~ 255°; Grexton 1995). North and south of the plateau regional ice-flow was towards the west, while in the west near Martin Hills, it was deflected northwesterly and southwesterly around it (Fig. 2; Fulton 1995). Throughout the Trout Lake region, a south to southwest directed ice-flow is consistently preserved by drumlins and fluting (Douglas 1959; Fulton 1995; Huntley et al. 2008).

The subsequent retreat of the ice-sheet broadly re-ordered the drainage systems across the CMV. Between 17-14 ka, the ice-margin on the Horn Plateau retreated towards the east, forming melt-water channels that eventually drained towards the west into an enlarged glacial Bulmer Lake (Huntley et al. 2006). After completely retreating from the Horn Plateau, the ice-margin continued to retreat (12-10 ka) in the Horn Plateau, creating even more meltwater channels with glaciofluvial deltas parallel to them (Huntley et al. 2006). Around the same time (12-11 ka), retreat of the ice-margin towards the north-northeast in the Trout Lake area shifted drainage from the southwest into glacial Lake Liard to the north into the CMV (i.e., glacial Lake Mackenzie; Huntley et al. 2008). Rapid retreat of the LIS continued between 11-10 ka, shifting the location of the glacial lakes and subsequent meltwater channels towards the east up the valley near Mills Lake (Duk-Rodkin and Lemmen 2000; Huntley et al. 2006). After ice retreat and final glacial lake drainage, modern fluvial drainage patterns were established, with post-glacial streams draining runoff and sediment radially from the Horn Plateau, Ebutt and Martin Hills into the Horn, Liard, Mackenzie and Willowlake river valleys

(Duk-Rodkin and Hughes 1994; Huntley et al. 2006). These major river valleys occupy previously established meltwater channels of the major Late Wisconsinan glacial lakes (Bulmer, Mackenzie, McConnell; Craig 1965; Huntley et al. 2006).

Our understanding of the CMV Quaternary history is further hampered by the nature of the cap bedrock. The soft, primarily Cretaceous and Devonian sedimentary rocks and pre-existing glacial deposits were prone to intense erosion, glacial deformation and ice-thrusting (e.g., Paulen 2009). As a result, most landforms and other evidence of earlier ice-flows were largely obliterated. Those that remained were extensively eroded, transported and re-deposited by colluvial, fluvial, lacustrine and aeolian processes during and following ice retreat. Other potential complexities in understanding the glacial transport and dispersal distance of KIMs in the CMV include palimpsest landscapes (e.g., Parent et al. 1996; Paulen 2013), ice streams (e.g., Margold et al. 2015) and regional subglacial meltwater storage and drainage events (e.g., Rampton 2000). Collectively, these many factors result in a complex and incomplete Quaternary history for the CMV.

Samples

In 2003 and 2005, a total of 325 heavy mineral concentrate stream sediment samples (~ 50 m^2 spacing) were collected in the Horn Plateau region by the Geological Survey of Canada (GSC; Day et al. 2007). GSC and Northwest Territories Geological Survey (NTGS) personnel followed this up in 2006 with the collection of 25 till samples weighing only 2-10 kg in the Horn Plateau region (Mills 2008). Meanwhile, 166 reconnaissance-scale till samples weighing ~ 10 kg each (~ 100 m^2 spacing) were collected from the Trout Lake region by the NTGS in 2008 (Watson 2010).

In total, 3665 (Horn Plateau) and 656 (Trout Lake) potential KIM grains were picked from the 0.25-2.0 mm size fractions and made into grain mounts. The Horn Plateau KIM inventory comprises peridotitic garnet (51 %), ilmenite (30 %), chromite (10 %), Cr-diopside (4 %), olivine (3 %), low-Cr (< 1 wt% Cr_2O_3) garnet (< 1 %) and rutile (< 1 %). The Trout Lake KIM inventory comprises rutile (45 %), peridotitic garnet (23 %), Cr-diopside (16 %), ilmenite (7 %), chromite (6 %), olivine (2 %) and low-Cr garnet (< 1 %). Sample descriptions, location, collection, heavy mineral concentrate processing and indicator mineral picking details are detailed elsewhere for the Horn Plateau (Day et al. 2007; Mills 2008) and the Trout Lake (Watson 2010). For sample descriptions and locations, the reader is referred to Tables S1-S3.

In addition, a collection of Mg-ilmenites from kimberlites with known emplacement ages ranging between ~ 700-30 Ma were used to try to constrain possible crystallization ages or age ranges of Horn Plateau Mg-ilmenites, based on their Hf isotope compositions. The large (1.0-2.0 mm size fraction) Horn Plateau Mg-ilmenite grains (n = 22) were selected based on necessary minimum Hf abundances needed for analysis (~ 0.5 ng). Samples used for Mg-ilmenite Hf isotopic analysis were provided as grain mounts, picked grains, hand samples or drill core. For a complete list of kimberlite sample localities, emplacement ages and kimberlite geochronology methods used for reference, the reader is referred to Table S4.

A database of KIM chemistry, primarily of peridotitic garnet, was used for comparison in this study. KIM chemistry for the Southwestern (Drybones Bay), Western (Aquila, Cross, Orion, Ursa), Southeastern (Snap Lake) and Central (Lac de Gras) Slave Craton kimberlites were used for comparison (Schulze et al. 1995; Carbno 2000; Kerr et al. 2000; Carbno and Canil 2002; Creaser et al. 2004; Griffin et al. 2004; Menzies et al. 2004; Aulbach et al. 2007, 2011; Roeder and Schulze 2008; Creighton 2009; Creighton et al. 2010; Bussweiler et al. 2015). The geochemical database has major element data as oxides (SiO_2, TiO_2, Al_2O_3, Cr_2O_3, FeO, MnO, MgO, CaO) as well as some trace element concentrations (e.g., Ni, Y, Zr, REEs for peridotitic garnet). In addition, a newly filtered (October 2017) NTGS GoData KIMC database was used to evaluate KIM chemistry from Central and Western Slave Craton surficial samples.

Methods

Sample preparation and elemental analysis

Picked indicator minerals from both regions were cleaned, mounted and analyzed for major and minor elements by electron probe microanalysis (EPMA), either previously at the GSC or during this study at the University of Alberta. EPMA analytical conditions, including standard information, are included in Supplementary Methodology. In total, 3153 Horn Plateau and 656 Trout Lake supposed KIM grains were analyzed. For complete KIM EPMA results see Tables S5-S10. Following EPMA, 947 peridotitic garnet grains and 53 peridotitic olivine grains from the study regions were analyzed for trace element abundances by in situ sector-field laser ablation inductively coupled mass spectrometry (LA-ICP-MS) at the University of Alberta. For LA-ICP-MS instrument setup, analytical conditions and standards used see Supplementary Methodology and Hardman et al. (this volume). For standard results, see Tables S11-S12 and Figures S3-S4. All external geochemical data were treated in the same way as the CMV KIM data, i.e., filtering of oxide totals, limits of detection, calculation of cations, garnet classification and thermobarometry techniques (e.g., Grütter et al. 2004; Nimis and Taylor 2000). Well-established methodologies for interpreting KIM chemistry were used to compare the Horn Plateau geochemical datasets with external data from potential source regions (i.e., Slave Craton kimberlites).

Isotopic analysis

Radiogenic isotopes were determined for select Trout Lake rutiles (U-Pb) and Horn Plateau Mg-ilmenite (Hf) to infer the age of eroded kimberlites that supplied the detrital kimberlitic material. Trout Lake rutiles grains (n = 53) were analyzed by LA-ICP-MS for U-Pb isotopic ratios (e.g., Malkovets et al. 2016) on a Thermo Element IIXR. For complete LA-ICP-MS rutile U-Pb dating instrument setup, analytical conditions and standards used see Supplementary Methodology and Harris et al. (this volume). For Trout Lake rutile U-Pb dating standard results, the reader is referred to Table S13 and Figure S5.

Nowell et al. (2004) have shown that Mg-ilmenite Hf isotope compositions potentially are a useful indicator of the broad emplacement age of their kimberlite source. Using a similar approach on Horn Plateau Mg-ilmenite grains (n = 22), we classify these kimberlitic ilmenite grains into potential age groups. We recognize that the rutile U-Pb ages offer a more precise technique (e.g., Cooper et al. 2008; Harris et al. this volume), however Mg-ilmenite Hf compositions are the only possibility of providing age constraints for the source kimberlites that supplied the Horn Plateau KIMs. In an attempt to better improve potential age constraints on Horn Plateau grains, the “kimberlite mantle Hf isotope evolution curve” defined by Mg-ilmenites was expanded and evaluated with the larger reference dataset of worldwide kimberlites, primarily from the North American Craton. Details of sample preparation, analysis using multi-collector (MC-)ICP-MS, analytical conditions and relevant reference material data are provided in Supplementary Methodology. For standard results, see Table S14 and Figure S6.

Geothermobarometry techniques

Thermobarometry of compositionally screened Cr-diopsides from garnet peridotites (criteria of Grütter 2009) were used to generate paleo-geotherms for each of the two study areas (using FITPLOT; Mather et al. 2011), based on the assumption that all KIM grains were sampled penecontemporaneously from their mantle sources. The mean temperature of the Ni-in-garnet thermometers of Griffin et al. (1989) and Canil (1999) was used to constrain the temperature of last equilibration of peridotitic garnet xenocrysts. If possible, the Ni-in-garnet temperatures were projected to their respective pyroxene-based geotherm. The Al-in-olivine thermometer for garnet peridotites (Bussweiler et al. 2017) was used to evaluate whether any different mantle sampling information is captured by olivine versus garnet. Similar to garnet temperatures, the Al-in-olivine temperatures were projected, if possible to their respective pyroxene-based geotherm.

Statistical analysis

Peridotitic garnet chemistry from Slave Craton kimberlites and the Horn Plateau populations overlap in many existing bivariate discrimination methods (e.g., Grütter et al. 2004). To investigate these populations statistically, we recast major element data as natural logarithm-normalized cation ratios for Ti, Al, Cr, Fe, Mn, Mg and Ca with Si as the denominator (e.g., ln(Ti/Si)). The natural logarithm permits elemental values to be expanded past the limited range created by the unit-sum constraint of geochemical data, shifts distributions closer to normality (Hardman et al. 2018) and helps alleviate problems with closure in geochemical data (Aitchison 1994). Peridotitic garnet chemistry populations from Horn Plateau and Slave Craton kimberlites and surficial samples were tested for normality via the Kolmogorov-Smirnov (K-S), Anderson-Darling (A-D) and Shapiro-Wilks (S-W) tests. These normality tests reject the hypothesis of normality when the p-value is ≤ 0.05. Failing the normality test allows you to state with 95 % confidence the data does not fit a normal distribution while passing the tests only allow you to state no significant departure from normality was found. Execpt for ln(Mn/Si) for the Western Slave Craton kimberlite population ($p = 0.09$), distributions of the Horn Plateau and Slave Craton peridotitic garnet populations are non-normal for all other elements ($p \leq 0.05$; Table S15).

Logistic regression (LR) was selected for comparison of our data with garnet chemistry from Slave Craton kimberlites, as it makes no underlying assumptions about distribution or normality. This non-parametric supervised statistical technique linearly transforms data, reduces dimensionality and maximizes the variance of multivariate datasets (Pohar et al. 2004). The LR solutions are derived using the freeware statistics package R using the following log-normalised variables (see Supplementary Methodology for run-stream): ln(Ti/Si), ln(Al/Si), ln(Cr/Si), ln(Fe/Si), ln(Mn/Si), ln(Mg/Si), ln(Ca/Si). Logistic regression solutions are derived for pairs of populations (e.g., the Horn Plateau and Central Slave), which results in a linear equation that assigns a numerical value to all data (Table S15). A density distribution of garnets in the populations based on these values is assessed for the degree of separation or overlap between different groups. The advantages and disadvantages of various statistical techniques are discussed in Supplementary Methodology.

Results: KIM chemistry

Cr-diopside

Major element variations of Cr-diopside grains from the Horn Plateau ($n = 138$) and Trout Lake ($n = 106$) indicate multiple petrogenetic sources (Fig. 3). Of these, 124 Horn Plateau and 19 Trout Lake grains have mg# (molar Mg/(Mg+Fe)) > 0.88 and elevated Cr_2O_3 (> 0.5 wt%) typical of mantle peridotites (Fig. 3). The mg# of Horn Plateau peridotitic Cr-diopsides is higher (mean of 0.92) compared to those from Trout Lake (mean of 0.90). Peridotitic Cr-diopsides from the Horn Plateau can be sub-divided into at least two different groups (criteria outlined by Ramsey and Tompkins 1994; Nimis 1998; Cookenboo and Grütter 2010). The first group contains 120 Horn Plateau and 15 Trout Lake Cr-diopside grains with lower Al_2O_3 (< 4 wt%) contents and generally higher mg# (mean 0.92), typical of Cr-diopside from garnet-peridotites (Fig. 3). The second group of peridotitic Cr-diopsides consists of four Horn Plateau and four Trout Lake Cr-diopside grains with higher Al_2O_3 (> 4 wt%) contents and variable mg# (0.89-0.95; Fig. 3). The grains from this group are either from off-craton garnet-peridotites or from spinel-peridotites (on- or off-craton). Most of the CMV peridotitic Cr-diopside grains are compositionally indistinguishable from those derived from Central and Western Slave Craton surficial samples (Fig. 3).

Low-Cr garnet

Of the 30 Horn Plateau low-Cr garnets analyzed, 20 are undefined (G0) and of potentially crustal origin, six are low-Cr megacrysts (G1), three are low-Ca eclogitic (G3) and two are high-Ca eclogitic to pyroxenitic (G4; after Grütter et al. 2004). The crust-mantle method of Hardman et al. (2018) classifies all four G3 and G4 grains as “mantle-derived” (Fig. S7). Out of 17 low-Cr garnet grains collected from the Trout Lake, nine classify as G3 with non-deemed “mantle-derived” using the Hardman et al. (2018) scheme (Fig. S7).

Peridotitic garnet

Of 1638 peridotitic garnet grains classified using the scheme of Grütter et al. (2004), from the Horn Plateau, lherzolitic garnets (G9) dominate (51 %), followed by high-TiO_2 peridotitic garnets (G11, 27 %), harzburgitic garnets (G10, 8 %) and wehrlitic garnets (G12, 5 %). A small portion of the Horn Plateau garnets are Cr_2O_3-rich (10-15 wt%) with only 3 % situated above the graphite-diamond constraint (Fig. 4; Grütter et al. 2006). Conversely, the Trout Lake peridotitic garnets are all G9 (n = 138), except for one G12 grain and generally plot in the high-Ca off-craton portion of the lherzolitic field (Grütter et al. 2004), setting them apart from typically lower Ca lherzolitic garnets from the Horn Plateau (Fig. 4).

Based on their chondrite-normalized rare earth element patterns (REE_N) patterns (Fig. 5), peridotitic garnets from the Horn Plateau can be classified in three principal groups (see Table S16). (1) HREE-enriched patterns have very low LREE concentrations that increase to chondritic abundances through the MREEs, becoming ~ 10x chondritic in the HREEs (Fig. 5). This is the largest group (55 % of the garnets) and is dominated by G9s (n = 309), followed by 127 G11, four G12 and three G10 grains. Based on their Ni contents, the HREE-enriched group covers the entire temperature range observed for Horn Plateau garnets and have variable Zr, Y, Hf abundances (Fig. S8). (2) Garnets from the MREE-depleted group have V-shaped to extremely sinusoidal REE_N patterns with variable, typically super-chondritic LREE abundances, decreasing concentrations from Ce or Nd to Tb or Ho and steep linear positive slopes in the $HREE_N$ with near chondritic Lu concentrations (Fig. 5). This group contains 13 G10, seven G11, five G12 and four G9 grains with Ni temperatures < 1100 °C for all garnets (except one). All garnets from this group have very low Zr, Y and Hf concentrations (< 0.024 ppm), at or below chondrite abundance (Fig. S8). (3) Garnet REE_N patterns of the sinusoidal group have positive slopes in the $LREE_N$ with a peak at Nd, negative slopes in the $MREE_N$ with a trough between Dy and Er and positive slopes in the $HREE_N$ (Fig. 5). This group consists of 202 G9, 73 G10, 48 G11 and 15 G12 grains with low and high Zr, Y and Hf concentrations, occurring in approximately equal proportions and again extending across the entire temperature range observed for Horn Plateau garnets (Fig. S8).

Olivine

Kimberlite-related (largely mantle-derived xenocrystic) olivine must be differentiated from that originating from "basaltic" sources recovered in surficial samples. Only 38 of the 109 Horn Plateau olivine grains have chemistry typical of xenocryst cores of olivine from kimberlites (mg# 0.89-0.94, NiO $\geq$ 0.3 wt%, CaO $\leq$ 0.1 wt%, MnO $\leq$ 0.15 wt%; e.g., Bussweiler et al. 2015, 2017). All 15 Trout Lake olivines fall within this mantle range, although they have a less variable, lower mg# (mean 0.91) compared to those from the Horn Plateau (mean mg# 0.92). A few olivine grains from the Horn Plateau (n = 13) and Trout Lake (n = 1) have compositions typical for olivine inclusions in diamond with mg# > 0.91 (Stachel and Harris 2008) and Cr_2O_3 < 0.03 wt% (Fipke et al. 1995).

Ilmenite

Kimberlite-derived ilmenite can be distinguished from non-kimberlitic magmatic ilmenites based on the TiO_2 versus MgO discrimination plot of Wyatt et al. (2004). Out of 46 Trout Lake ilmenite grains, only four are kimberlitic (i.e., plot to the right of the discriminant curve in Fig. 6) whereas ilmenites from the Horn Plateau are more promising for diamond exploration, with 793 grains (of 948) being of kimberlitic composition.

Mills (2008) noted that Horn Plateau Mg-ilmenites document a complex crystallization history with both Cr_2O_3- and MgO-poor (oxidized) and Cr_2O_3- and MgO-rich (reduced) suites which define two groups: (1) a less prominent group with 5-7 wt% MgO and very low Cr_2O_3 and (2) a dominant group with > 10 wt% MgO and Cr_2O_3 increasing with MgO-content. All four kimberlitic Mg-ilmenite grains from three Trout Lake samples have similar Nb_2O_5, TiO_2, Cr_2O_3, MnO and MgO contents to the Cr_2O_3- and MgO-poor suite of the Horn Plateau. These four Trout Lake grains and 10-25 % of the Horn Plateau Mg-ilmenites are characterized by relatively low TiO_2, MgO and Cr_2O_3 values that increase at the low end of the MgO-spectrum, similar to those from the Drybones Bay kimberlite (Fig. 6; Schulze et al. 1995; Kerr et al. 2000). Meanwhile, the majority of Horn Plateau grains (75-90 %) have similar Nb_2O_5, TiO_2, Cr_2O_3, FeO and MgO contents as those from Western and Central Slave Craton surficial samples (Fig. 6).

Rutile

Although some studies have attempted to recognize kimberlite-related rutiles based on chemical composition (e.g., based on Cr_2O_3 contents; Malkovets et al. 2016), other studies of rutile from mantle xenoliths show that major elements are less definitive (Harris et al., this volume). CMV rutiles also allow no clear distinction (Table S10). None of the Trout Lake rutiles (n = 291) contain ≥ 1.7 wt% Cr_2O_3, thought to be typical of a cratonic mantle source, while none of the four Horn Plateau rutiles contain > 0.4 wt% Cr_2O_3, thought to be necessary for distinction from crustal sources (Fig. S9; Malkovets et al. 2016).

Only rutile from Trout Lake samples were analyzed for U-Pb isotope systematics and most grains have extremely low ^{207}Pb concentrations (in addition to Th and U), as is especially common for accessory minerals (e.g., rutile, zircon) from Mesozoic or younger magmas (e.g., Zack et al. 2011). Thus, accurate $^{207}Pb/^{235}U$ ages were difficult to obtain and only the $^{206}Pb/^{238}U$ ratios and apparent ages (Table S17), which have the lowest analytical uncertainties, were considered for resolving the emplacement age of eroded kimberlites that supplied these detrital rutile grains.

Trout Lake rutile $^{206}Pb/^{238}U$ ages can be divided into three distinct groups: (1) two grains (4 %) with Archean $^{206}Pb/^{238}U$ ages similar to Slave Craton granitoid rocks (2.8-2.5 Ga), (2) 47 grains (89 %) with Proterozoic $^{206}Pb/^{238}U$ ages similar to the Wopmay Orogen rocks (2.1-1.6 Ga) and (3) four grains from three samples (8 %) with potential kimberlitic $^{206}Pb/^{238}U$ ages between 429-138 Ma (Fig. S10), based on the lack of evidence for metamorphic events of such young ages in the CMV basement. Of these presumed kimberlitic rutile grains, the two oldest have Silurian and Early Devonian $^{206}Pb/^{238}U$ ages of 420.6 ± 8.2 Ma and 408.1 ± 11 Ma (Silurian and Early Devonian). These two rutile grains are from separate samples where they occur with other rutiles defining Paleoproterozoic crystallization ages (Fig. S10). Meanwhile the two youngest kimberlitic rutile grains, again from two separate samples, have Late Triassic to Early Cretaceous $^{206}Pb/^{238}U$ ages of 144.6 ± 6.2 Ma and 227.0 ± 35 Ma (2σ; Fig. S10).

Spinel

At least 70 % of the Horn Plateau (n = 314 total) and only 12 % of the Trout Lake (n = 42 total) spinels have major element compositions (TiO_2, Al_2O_3, Cr_2O_3, MgO) typical of spinels from kimberlites (e.g., Sobolev 1977). On the basis of cr# vs mg# systematics (Roeder and Schulze 2008), potential Horn Plateau KIM grains with typically low mg# (< 0.35) and moderate cr# (0.4 to 0.8) are indistinguishable from spinels from Central and Western Slave Craton surficial samples (Fig. S11).

Discussion

Geothermobarometry

The Horn Plateau Cr-diopsides (n = 54) define a conductive paleo geotherm equivalent to a lithospheric thickness of 200 (± 10) km (Fig. 7), assuming a mantle potential temperature of 1300 °C. Although the possibility that this geotherm represents mixed datasets (Cr-diopsides from various sources) cannot be excluded, the tight correlation (Fig. 7) makes it highly unlikely that sources with significantly variable geotherms could have been sampled. This geotherm has a wide "diamond window" (Fig. 7) and with increasing depth crosscuts the 35-38 mW/m^2 model geotherms of Hasterok and Chapman (2011). Meanwhile, only three Trout Lake Cr-diopside grains passed compositional screening; they cluster in a narrow pressure-temperature interval within the graphite stability field and do not allow for the derivation of a reliable paleogeotherm (Fig. 7).

Of the 808 peridotitic garnet grains analyzed for trace elements from the Horn Plateau, the majority have Ni-in-garnet temperatures between 850-1350 °C (Fig. S8; Tables S16, S18); while the 138 G9 grains from the Trout Lake extend to lower temperatures spanning a smaller range, between 800-1050 °C (except one grain; Table S19). Projection of Ni-in-garnet temperatures to the pyroxene-based geotherm for Horn Plateau indicates significant sampling in the diamond stability field (Figs. 7 and 8). Based on the P_{38} Cr-in-garnet barometer of Grütter et al. (2006), a minimum (as presence of Mg-chromite in the assemblage cannot be confirmed) maximum pressure of 5.8 GPa can be derived for the most Cr-rich Horn Plateau garnets, equivalent to a minimum lithospheric thickness of ~ 180 km (Fig. 4). This result agrees with the intersection of the pyroxene-based geotherm for Horn Plateau with the mantle adiabat at 200 ± 10 km (Fig. 7). The lack of a reliable geotherm for the Trout Lake precludes projection of Ni-in-garnet temperatures to depth.

Application of the Al-in-olivine thermometer requires screening out of olivines from spinel- and garnet-spinel facies peridotites, as the thermometer is only confirmed to work in garnet-facies peridotites. Based on their position on the Al versus V plot for garnet versus spinel facies discrimination (Fig. S12), only 17 of 38 Horn Plateau olivines classify as garnet-peridotite-derived. All 15 Trout Lake olivine grains classify as garnet-peridotite-facies (Fig. S12; Table S20). Al-in-olivine temperatures for 16 of the garnet peridotite-derived olivine grains from Horn Plateau are between 950-1200 °C (see Table S18). Projection of these Al-in-olivine temperatures to the Horn Plateau paleogeotherm (Fig. 7) indicates that they most recently equilibrated at or deeper-than the graphite-diamond transition (Day 2012) with a similar mode in sampling depth as that defined by the garnets (120-180 km; Fig. 8). The Al-in-olivine temperatures for the 15 Trout Lake garnet-peridotite derived olivine grains are much higher (1000-1350 °C) than the temperature obtained from garnet-peridotite derived Cr-diopsides at Trout Lake (650-750 °C).

Diamond potential of KIMs

Pyroxene-based geothermobarometry for Horn Plateau KIMs indicates derivation from a cold, deep (190-210 km) lithospheric mantle root, with a large diamond window that was abundantly sampled (Figs. 7-8). For Trout Lake, the lack of a pyroxene-based geotherm makes it difficult to interpret the thickness of lithosphere sampled by the kimberlite sources of the sampled indicators. The three pressure-temperature estimates based on Cr-diopside grains from this area, however, plot close to the Horn Plateau model-geotherm (Fig. 7) suggesting it is not significantly different from that for the Horn Plateau Cr-diopside grains.

Cr_2O_3-CaO contents of peridotitic (≥ 1 wt% Cr_2O_3) garnets analyzed from both study areas (Fig. 4) suggest significantly different compositions of lithosphere sampled and transported to the surface. For Horn Plateau, the peridotitic garnet chemistry suggests derivation from thick and highly depleted lithosphere that extends into the diamond stability field. In stark contrast, for Trout Lake, both the absence of G10 garnets and the overall lower Ni-in-garnet temperatures suggest shallower sampling of a less depleted lithospheric section, likely with less favourable diamond potential.

All four Trout Lake Mg-ilmenites and a smaller portion of Horn Plateau grains (10-25 %) with low Cr_2O_3 and MgO contents (Fig. 6) have elevated Fe^{3+}/Fe^{2+} ratios (calculated from stoichiometry) that indicate less favourable redox conditions for diamond preservation (e.g., Schulze et al. 1995). Castillo-Oliver et al. (2017), however, questioned the utility of Fe-Mg systematics in Mg-ilmenite in defining diamond preservation potential. The extremely Cr_2O_3-rich Mg-ilmenite grains from the "reducing" suite (75-90 %) are suggested to indicate a very depleted and Cr-rich mantle source with favourable diamond potential (Mills 2008 and references therein). Moreover, 10 Horn Plateau (and no Trout Lake) spinels have > 61 wt% Cr_2O_3, 10-16 wt% MgO, < 0.60 wt% TiO_2, < 8 wt% Al_2O_3, < 6 wt% Fe_2O_3, 13-17 wt% FeO (Fe contents calculated based on stoichiometry), i.e., compositions typical of diamond inclusion spinels (e.g., Sobolev 1977; Fipke et al. 1995) and hence indicative of favourable diamond potential.

Based on our new data and including previous studies on KIMs from Horn Plateau and Trout Lake (Day et al. 2007; Mills 2008; Pitman 2014), we conclude that Horn Plateau appears to have excellent diamond potential (provided that the indicator sources are local) while Trout Lake does not provide a viable exploration target.

Potential source ages of Horn Plateau KIMs

Although the relationship between ilmenite Hf isotope composition and kimberlite emplacement age is scattered and hence imprecise, it is very useful in allowing, e.g., to distinguish between Neoproterozoic-Silurian kimberlites and those of Devonian-Paleogene ages (Fig. 9, bottom). Based on the current worldwide kimberlitic ilmenite dataset (Fig. 9, bottom), Horn Plateau Mg-ilmenite Hf isotope compositions can be broadly divided into two age groups (Table S21).

The older age group contains nine Mg-ilmenites (from eight samples) with less radiogenic and restricted $^{176}Hf/^{177}Hf$ ratios between 0.2825-0.2826, indicative of Neoproterozoic to Silurian kimberlite emplacement ages (Fig. 9). All the Mg-ilmenites of the older age group belong to the Cr_2O_3- and MgO-poor oxidizing suite at Horn Plateau (Fig. 6), as outlined by Mills (2008), with similar Nb_2O_5, TiO_2, Cr_2O_3, FeO and MgO contents as those from the Drybones Bay kimberlite (Fig. 6; Schulze et al. 1995; Kerr et al. 2000). The younger age group contains 12 Mg-ilmenites (from 10 samples) with more radiogenic and less restricted $^{176}Hf/^{177}Hf$ ratios of 0.2827 to 0.2831, indicative of Devonian to Paleogene kimberlite emplacement ages (Fig. 9). All younger age Mg-ilmenites lie within the dominate MgO- and Cr_2O_3-rich suite outlined at Horn Plateau by Mills (2008), with similar Nb_2O_5, TiO_2, Cr_2O_3, FeO and MgO contents as those from Central and Western Slave Craton surficial samples (Fig. 6).

Horn Plateau KIM populations

Results from this study support the conclusions of previous studies (e.g., Mills 2008) which suggested that the Horn Plateau KIMs are derived from multiple (at least one proximal and one distal) kimberlite sources. Mg-ilmenites define at least two groups based on distinct compositions and ages (Neoproterozoic-Silurian versus Devonian-Paleogene). The large variability in Hf isotope ratios clearly precludes that the Mg-ilmenites came from a single kimberlite field of restricted age.

Peridotitic garnet major element chemical data from the Horn Plateau has a non-normal distribution for all major and minor elements. This is typical for regional geochemical data, even after logarithmic transformation and suggests the likelihood of mixing from multiple kimberlite sources (e.g., Reimann and Filzmoser 2000). Garnet chemistry from the NTGS GoData data base for Slave Craton surficial samples also reveals widely varying, non-normal compositional characteristics suggesting they are also from multiple sources.

Variations in KIM chemistry with geographic location, as can be observed in the Horn Plateau (Day et al. 2007; Mills 2008) and HOAM property mineral chemistry data (Pitman 2014), also suggest mixing of KIMs from multiple sources. Mg-ilmenites recovered from till samples (four grains from three samples) on the Horn Plateau are evenly split into the two compositional/age groups previously outlined. Surficial samples principally containing Mg-ilmenites of the younger age group were collected from primary or secondary streams with moderate to good drainage, either on or near the edge of the Horn Plateau, suggesting they are sourced from the top of the plateau. Whether this source on the Horn Plateau is primary or secondary remains to be proven. The two stream sediment samples containing Mg-ilmenite grains with Hf isotope compositions from both age groups were taken from tertiary streams north of the Horn Plateau, along an ancient meltwater channel, suggesting at least two kimberlite sources have been mixed within this region.

Potential sources of Horn Plateau KIM populations

A key question is whether these Horn Plateau KIM populations were derived from proximal kimberlites within the CMV/Horn Plateau or distal sources, for instance, from diamondiferous kimberlites on the Slave Craton. Following the discovery of economic diamondiferous kimberlites in the Lac de Gras area, it was thought that the Horn Plateau KIMs were glacially transported south-westward from the Central Slave Craton (e.g., Day et al. 2007; Mills 2008 and references therein). Besides distinct similarity in the excellent diamond potential indicated by Horn Plateau KIM major element chemistry to the Central Slave Craton data set, one of the main arguments for a distal origin was the large amount of glacial debris, including granitic boulders of presumed Slave Craton origin, throughout the CMV (Day et al. 2007; Mills 2008). Most of these granitic glacial erratics have, however, not been dated, leaving the possibility that they may derive from more proximal source regions, such as the Wopmay Orogen.

The logistic regression (LR) solutions for peridotitic garnet chemistry from the Horn Plateau and kimberlites and surficial samples from the Central Slave Craton show sufficient spread in the population density distributions (Fig. 10) to reliably distinguish Horn Plateau and Central Slave Craton derived KIMS where the populations do not strongly overlap. Based on the major element datasets analyzed using LR, it is likely that at least part of the Horn Plateau KIMs were not derived from the Central Slave Craton, as their population density distributions have solutions which do not overlap (Fig. 10). There is, however, significant overlap between peridotitic garnets from the Horn Plateau and surficial samples and kimberlites from the Western Slave Craton in their respective LR solution (Fig. 10). Consequently, the two populations cannot be probabilistically discriminated using LR and hence we cannot reject the possibility that the Horn Plateau KIMs were derived from the Western Slave Craton. In context of the inferences we draw from these LR results and other KIM chemistry results, we explore potential kimberlite sources of the Horn Plateau KIMs.

Central Slave Craton kimberlites

The Central Slave Craton kimberlites (> 500 km northeast of the Horn Plateau) were emplaced largely between Late Cretaceous to Eocene times (75-45 Ma; Heaman et al. 2003; Creaser et al. 2004; Sarkar et al. 2015). These kimberlites could be the source of the younger Horn Plateau Mg-ilmenite group. Nine of the 12 analyzed Mg-ilmenites from this age group have $^{176}Hf/^{177}Hf$ ratios that overlap with ilmenites from Diavik and Ekati kimberlites (Fig. 9; Table S21). In addition, Cr-diopside chemistry (Fig. 3) and pressure-temperature estimates (Fig. 8) and peridotitic garnet major, minor and trace element chemistry (Figs. 4-5) are remarkably similar to those from the Central Slave Craton kimberlites dataset.

Paleogeographic reconstructions indicate fluvial systems transported eroded detritus away from the CMV, east across the Slave Craton towards Hudson Bay, during the Paleogene and Neogene (Duk-Rodkin and Hughes 1994; Dixon 1999; Duk-Rodkin and Lemmen 2000), which rules out fluvial transport of kimberlitic material from these kimberlites into the CMV. Quaternary transport by glacial (-fluvial) activity is the only possible mechanism for transporting material from these kimberlites towards the southwest into the Horn Plateau. Mg-ilmenites from till samples in the eastern Horn Plateau (Last Stop Claims; n = 56) are all from the MgO- and Cr_2O_3-rich suite, suggesting the source of the "younger" (reduced) Mg-ilmenite age group may be outside the CMV, to the northeast. However, studies of indicator mineral glacial dispersal trains/fans indicate typical maximum transport distances of up to 180-200 km (e.g., McClenaghan et al. 2002; McClenaghan 2005) making transport of large concentrations of kimberlitic material (even kimberlitic boulders) from these kimberlites over large distances very unlikely. Ice streams could have influenced dispersal of Horn Plateau KIMs (e.g., Margold et al. 2015), although there is no field evidence for these features to the east-northeast of the Horn Plateau region or the Slave Craton.

Distinct spinel major element chemistry variations and lack of eclogitic garnets (G3) and megacrysts (G1) relative to Central Slave Craton kimberlites, led Mills (2008) to suggest Ekati Lease Block (Lac de Gras area) kimberlites are not the source of the Horn Plateau KIMs. In addition, the re-constructed lithospheric stratigraphy of Horn Plateau garnets is slightly different to that of Central Slave Craton kimberlites; specifically, the Horn Plateau KIM data lacks the distinct ultra-depleted shallow (120-150 km) "layer" chemistry that characterises the mantle beneath that region (e.g., Griffin et al. 1999; Menzies et al. 2004). Further, > 20 % of the Horn Plateau G10 grains equilibrated at depths ≥ 150 km (> 1000 °C; Fig. S8; Table S18), whereas relatively few G10s from the Central Slave lithosphere, in published datasets (e.g. Grütter et al. 1999), have yielded depths deeper than the ultra-depleted shallow layer (i.e., ≥ 150 km or > 1000 °C).

HOAM project Liard properties kimberlites

Besides the HOAM project kimberlites > 20 km southwest of the Horn Plateau and directly north-northwest of Trout Lake (Fig. 1), there are no other known kimberlites in the vicinity with possible Devonian to Paleogene emplacement ages. Olivut Resources Ltd. report intersecting 29 kimberlites (two diamondiferous) from 39 drill holes on their Liard properties (Pitman 2014), with uppermost diatreme and possibly crater facies (kimberlitic breccias and tuffs), as well as deeper root zone features (hypabyssal facies and abundant dikes) indicated. The locations and depths of drill holes that intersected kimberlites in the Liard properties (Figs. 1; Pitman 2014) when correlated with bedrock stratigraphy suggest Early to Late Devonian kimberlite emplacement ages.

One of the Devonian-Paleogene age Mg-ilmenite grains with the lowest $^{176}Hf/^{177}Hf$ ratio from this group, was recovered just south of the Mackenzie River. This sample collected alluvium from the same watershed that hosts HOAM project kimberlites (< 10 km south; Fig. 2). The other Devonian-Paleogene age Mg-ilmenite grain (17961-011) with a similar $^{176}Hf/^{177}Hf$ ratio within uncertainty (see Table S21) was collected approximately 120 km northwest of HOAM project kimberlites (near Ebutt Hills), parallel with regional ice-flow directions. Correlations between the two samples containing these younger age group Mg-ilmenites with the glacial transport direction (Fig. 2) and distance from the HOAM project kimberlites suggest these two grains are likely sourced from these kimberlites.

Southwestern and Western Slave Craton kimberlites

The Silurian Southwestern (Drybones Bay) and Ordovician Western Slave Craton kimberlites (Fig. 1) have emplacement ages consistent with the older age Mg-ilmenites (Fig. 9), suggesting possible derivation from kimberlites from these general areas. KIM chemistry from surficial samples in the immediate area to the Drybones Bay kimberlite indicate other undiscovered kimberlites likely exist (Kerr et al. 2000). The older age Horn Plateau Mg-ilmenites, as well as some of the other KIMs, have similar major and minor chemistry to grains from the Drybones Bay kimberlite and some of the Western Slave Craton surficial samples (Figs. 3, 4, 6, S8).

Present lithosphere thicknesses of 180-200 km, inferred from seismic tomography for the Southwestern and Western Slave Craton (Fig. 1; Schaefer and Lebedev 2014), are nearly identical to lithosphere thickness estimates based on Horn Plateau Cr-diopside (190-210 km; Fig. 7). Viable transport mechanisms (glacial and/or fluvial), distances (< 300 km) and directions (west-southwest), as well as KIM chemistry similarities suggest some of the Horn Plateau KIMs could be sourced from kimberlites in the Western and/or Southwestern Slave Craton areas. Further details of chemical traits between these possible sources, as well as discussion of viable transport mechanisms of KIMs can be found in the Supplementary Discussion.

Undiscovered Horn Plateau region kimberlites

Nine younger age Horn Plateau Mg-ilmenites are found on the Horn Plateau itself or in streams directly draining it where till domains with proximal clast lithology are indicated (Mills 2008 and references therein). In direct proximity to these samples near Willow Lake (Fig. S1), below the overburden, Aptian-Albian-aged sediments are preserved, which could host primary source kimberlites for these KIMs. Another viable region for primary source kimberlites for the younger age Horn Plateau KIMs are within Campanian-Maastrichtian clastic sediments, which lie below overburden on the southern portion of the Horn Plateau (Fig. S1). These two regions with preserved Cretaceous sediments have similar present-day lithospheric thicknesses (180-200 km based on seismic tomography; Fig. 1), in perfect agreement with the lithosphere thickness (190-210 km; Fig. 7) derived from Horn Plateau Cr-diopsides.

The largest quantities of analyzed peridotitic garnets, with extremely high proportions of Ni-in-garnet temperatures > 950 °C, are found in samples proximal (< 25 km) to these Cretaceous clastic sediments on the southern and eastern portions of the Horn Plateau (Fig. S13). Derived from the same watershed are 14 grains (from 13 samples) giving Al-in-olivine temperatures between 950-1100 °C and 17 Cr-diopsides grains (from 12 samples) with temperatures all > 950 °C (Fig. S13). This area coincides with the north-trending Bulmer Lake gravity high (Fig. 1), which is suspected to be a Precambrian faulted contact that was re-activated during the Late Cretaceous. Seismic surveys also indicate dominant northeast-trending and subsidiary northwest-trending faults that were also likely re-activated during this time (Aitken 1993; Gal and Lariviere 2004 and references therein). Such faults may have facilitated kimberlite emplacement in the Horn Plateau region.

This same area on top of the Horn Plateau could also be a secondary (sedimentary) source region for the older age KIM population(s). In addition, sub-cropping below moderately thick glacial deposits (50-80 m; Cragie 1991), Cambrian-Silurian aged sedimentary rocks to the north-northeast of the Horn Plateau, near Lac la Martre (north of ~ 62 °N), could host primary kimberlites and/or be a secondary source of the older age Horn Plateau Mg-ilmenite group, as they lie directly up-ice of regional ice-flow directions (~ 100 km northeast of the Horn Plateau).

Conclusions

Analysis of KIMs from two Central Mackenzie Valley study areas has resulted in a large, new geochemical dataset for an underexplored area of the Northwest Territories. These geochemical data provide new constraints on the diamond potential for future exploration within the area. The kimberlitic source of the KIMs from the Trout Lake region sampled shallow portions of lithospheric mantle although no constraints on the depth of the lithosphere can be made from current results. In contrast, KIMs from the Horn Plateau region have significant diamond potential, with a relatively high proportion of harzburgitic diamond-facies (G10D) garnets and many of the analyzed KIMs deriving from the diamond stability field. A ca. 200 km thick lithosphere beneath the kimberlites sourcing the Horn Plateau kimberlites, as determined from clinopyroxene thermobarometry, is at least consistent with present-day seismology constraints (Fig. 1).

Single grain Hf isotope analyses of Mg-ilmenites from the Horn Plateau show a wide variety of isotopic compositions indicating at least two major age populations in their source kimberlites. These results are consistent with past major-element based studies of Horn Plateau KIMs that suggested the grains were likely sourced from at least two kimberlitic sources (one proximal and one distal) based on their grain morphology, major element chemistry and dispersion patterns (Day et al. 2007; Mills 2008). Comparative geochemistry and statistical tests, coupled with KIM surface textures (Mills 2008), till lithology domains (Mills 2008), pre-glacial bedrock distributions (Meijer Drees 1993; Duk-Rodkin et al. 1994) and ice-flow records (Fulton 1995), allow us to exclude some Slave Craton kimberlites (specifically the Lac de Gras field) as the only possible sources of Horn Plateau KIMs and instead highlight the southern/western Slave Craton area as a potential source for some of the KIMs. The KIM populations are, however, clearly mixed and permit more local sources. The incompletely resolved Quaternary history of the area remains a primary obstacle to locating the kimberlitic source(s) of the proximal, potentially “younger” Horn Plateau KIM population(s). Until Horn Plateau chromite, peridotitic garnet and olivine populations can be distinguished from other Southwestern and/or Western Slave Craton kimberlites, the potential for undiscovered kimberlites within the CMV remains possible and even likely.

Acknowledgements The authors gratefully acknowledge the permission of the NTGS to publish this data and are grateful for funding student salary and analytical costs associated with this research project. The remainder of funding was provided by an NSERC CREATE grant to Pearson (Grant # 479905-2016). We thank the NTGS, Peregrine Diamonds, Diavik Diamond Mines and Dominion Diamonds for supplying ilmenites for Hf isotope characterization. Andrew Schaefer is thanked for his seismic tomography cross-sections. This manuscript was significantly improved by reviews from Bruce Kjarsgaard and Curtis Brett. The authors also thank Andrew Locock, Chiranjeeb Sarkar, Martin Von Dollen, Mark Labbe, Yannick Bussweiler and Yan Luo for valuable guidance and discussions regarding analytical techniques and publishing the data.

References

Aitchison J (1994) Principles of compositional data analysis. Multivariate Analysis and its Applications. IMS Lecture Notes – Monograph Series 24: 73-81

Aitken JD (1993) Proterozoic sedimentary rocks; Subchapter 4A. In: Stott DF, Aitken JD eds., Sedimentary Cover of the Craton in Canada. Geological Survey of Canada, Geology of Canada, 5:81-95

Aspler LB, Pilkington M, Miles WF (2003) Interpretation of Precambrian Basement based on recent aeromagnetic data, Mackenzie Valley, Northwest Territories. Geological Survey of Canada, Current Research 2003-C2

Aulbach S, Pearson NJ, O'Reilly SY, Doyle BJ (2007) Origins of xenolithic eclogites and pyroxenites from the Central Slave Craton, Canada. Journal of Petrology 48:1843-1873

Aulbach S, Stachel T, Heaman LM, Carlson JA (2011) Microxenoliths from the Slave craton: Archives of diamond formation along fluid conduits. Lithos 126:419-434

Burwash RA, Green AG, Jessop AM, Kanasewich ER (1993) Geophysical and petrological characteristics of the basement rocks of the Western Canada Basin; Chapter 3. In: Stott DF, Aitken JD eds. Sedimentary Cover of the Craton in Canada. Geological Survey of Canada, Geology of Canada, 5:55-77

Bussweiler Y, Foley SF, Prelević D, Jacob DE (2015) The olivine macrocryst problem: new insights from minor and trace element compositions of olivine from Lac de Gras kimberlites, Canada. Lithos 220:238-252

Bussweiler Y, Brey GP, Pearson DG, Stachel T, Stern RA, Hardman MF, Kjarsgaard BA, Jackson SE (2017) The aluminum-in-olivine thermometer for mantle peridotites—Experimental versus empirical calibration and potential applications. Lithos 271:301-314

Canil D (1999) The Ni-in-garnet geothermometer: calibration at natural abundances. Contributions to Mineralogy and Petrology 136:240-246

Carbno GB (2000) Geochemical and petrological interpretation of mantle structure beneath the southwest Slave Province, NWT. PhD, University of Victoria

Carbno GB, Canil D (2002) Mantle structure beneath the SW Slave craton, Canada: constraints from garnet geochemistry in the Drybones Bay kimberlite. Journal of Petrology 43:129-142

Castillo-Oliver M, Melgarejo JC, Galí S, Pervov V, Gonçalves AO, Griffin WL, Pearson NJ, O'Reilly SY (2017) Use and misuse of Mg- and Mn-rich ilmenite in diamond exploration: a petrographic and trace element approach. Lithos 293:348-363

Cook FA, Erdmer P (2005) An 1800 km cross section of the lithosphere through the northwestern North American plate: lessons from 4.0 billion years of Earth’s history. Canadian Journal of Earth Sciences, 42:1295-1311

Cook FA, van der Velden AJ, Hall KW, Roberts BJ (1999). Frozen subduction in Canada’s Northwest Territories: lithoprobe deep lithospheric reflection profiling of the Western Canadian Shield. Tectonics, 18:1-24

Cookenboo HO, Grütter HS (2010) Mantle-derived indicator mineral compositions as applied to diamond exploration. Geochemistry: Exploration, Environment, Analysis 10:81-95

Cooper SA, Belousova EA, Griffin WL, Morris BJ (2008) Age of FS66 kimberlite beneath Murray basin, South Australia: laser ablation ICP-MS dating of kimberlitic Zircon, Perovskite, and Rutile. Extended abstract 9th International Kimberlite Conference, Frankfurt, 9IKC-A-00106

Craig BG (1965) Glacial Lake McConnell, and the surficial geology of parts of Slave River and Redstone River map-areas, District of Mackenzie. Geological Survey of Canada, Bulletin 122

Craigie ER (1991) Diamond drill data, Horn River project, April 9-August 16, 1990. NWT Assessment File Report 083067

Creaser RA, Grütter H, Carlson J, Crawford B (2004) Macrocrystal phlogopite Rb–Sr dates for the Ekati property kimberlites, Slave Province, Canada: evidence for multiple intrusive episodes in the Paleocene and Eocene. Lithos 76:399-414

Creighton S (2009) The influence of mantle metasomatism on the oxidation state of the lithospheric mantle. PhD, University of Alberta

Creighton S, Stachel T, Eichenberg D, Luth RW (2010) Oxidation state of the lithospheric mantle beneath Diavik diamond mine, Central Slave craton, NWT, Canada. Contributions to Mineralogy and Petrology 159:645-657

Davis WJ, Ootes L, Newton L, Jackson VA, Stern RA (2015) Characterization of the Paleoproterozoic Hottah terrane, Wopmay Orogen using multi-isotopic (U-Pb, Hf and O) detrital zircon analyses: an evaluation of linkages to northwest Laurentian Paleoproterozoic domains. Precambrian Research, 269:296-310

Day HW (2012) A revised diamond-graphite transition curve. American Mineralogist 97:52-62

Day SJA, Lariviere JM, McNeil RJ, Friske PWB, Cairns SR, McCurdy MW, Wilson RS (2007) National Geochemical Reconnaissance: regional stream sediment and water geochemical data, Horn Plateau area, Northwest Territories (Parts of NTS 85E, 85F, 85K, 85L, 95H, 95I and 95J) including analytical, mineralogical and kimberlite indicator mineral data. GSC Open File 5478 / NWT Geoscience Office Contribution 0027

Dixon J. Mesozoic-Cenozoic stratigraphy of the northern Interior Plains and plateaux, Northwest Territories. Bull./Canada. Geol. survey. 1999.

Douglas RJW (1959) Great Slave and Trout River map-areas, Northwest Territories. Geological Survey of Canada, Paper 58-11

Duk-Rodkin A, Hughes OL (1994) Tertiary-Quaternary drainage of the pre-glacial Mackenzie Basin. Quaternary International 22:221-241

Duk-Rodkin A, Lemmen DS (2000) Glacial history of the Mackenzie region. In: LD Dyke and GR Brooks (eds.) The Physical Environment of the Mackenzie Valley, Northwest Territories: a Base Line for the Assessment of Environmental Change, pp 11-20

Fipke CE, Gurney JJ, Moore RO (1995) Diamond exploration techniques emphasising indicator mineral geochemistry and Canadian examples. Bulletin/Geol survey of Canada Dep. of natural resources

Fulton RJ (1995) Surficial Materials of Canada. GSC Map 1880A, GSC, Ottawa

Gal LP, Lariviere JM (2004) Edéhzhíe Candidate Protected Area Non-Renewable Resource Assessment (Phase 1) Northwest Territories, Canada, NTS 085E-FKL and 095H-IJ. NWT Open File 2004-01

Ghaznavi A, Taylor B, Henry JB (1986) Geophysical Exploration Report, Fort Simpson Survey, Northwest Territories. Exploration Agreement No. 166 by Petro-Canada Inc. National Energy Board Open File Report 9229-P028-006E

Grexton L (1995) 1993-1994 Regional Diamond Exploration Compilation Report on Geochemical and Geophysical Surveying, NTS 85L. NWT Assessment File Report 083528

Griffin WL, Cousens DR, Ryan CG, Sie SH, Suter GF (1989) Ni in chrome pyrope garnets: a new geothermometer. Contributions to Mineralogy and Petrology 103:199-202

Griffin WL, Doyle BJ, Ryan CG, Pearson NJ, Suzanne YO, Davies R, Kivi K, Van Achterbergh E, Natapov LM (1999) Layered mantle lithosphere in the Lac de Gras area, Slave Craton: composition, structure and origin. Journal of Petrology 40:705-727

Griffin WL, O'Reilly SY, Doyle BJ, Pearson NJ, Coopersmith H, Kivi K, Malkovets V, Pokhilenko N (2004) Lithosphere mapping beneath the North American plate. Lithos 77:873-922

Grütter HS (2009) Pyroxene xenocryst geotherms: Techniques and application. Lithos 112:1167-1178

Grütter HS, Apter DB, Kong J (1999) Crust-mantle coupling: evidence from mantle-derived xenocrystic garnets. In: Gurney JJ, Gurney JL, Pascoe MD, Richardson SH (eds) The JB Dawson Volume, Proceedings of the VIIth International Kimberlite Conference, vol. Red Roof Design, Cape Town, pp 307-313

Grütter HS, Latti D, Menzies A (2006) Cr-saturation arrays in concentrate garnet compositions from kimberlite and their use in mantle barometry. Journal of Petrology 47:801-820

Grütter HS, Gurney JJ, Menzies AH, Winter F (2004) An updated classification scheme for mantle-derived garnet, for use by diamond explorers. Lithos 77:841-857

Hardman MF, Pearson DG, Stachel T, Sweeney RJ (2018) Statistical approaches to the discrimination of crust- and mantle-derived low-Cr garnet – Major-element-based methods and their application in diamond exploration. Journal of Geochemical Exploration 186:24-35

Hardman MF, Pearson DG, Stachel T, Sweeney RJ (2018) Statistical approaches to the discrimination of mantle- and crust-derived low-Cr garnets using major and trace element data. Miner Petrol, this volume

Harris GA, Pearson DG, Liu J, Hardman MF, Snyder DB, Kelsch D (2018) Mantle Composition, Age and Geotherm beneath the Darby Kimberlite field, West Central Rae Craton. Miner Petrol, this volume

Hasterok D, Chapman DS (2011) Heat production and geotherms for the continental lithosphere. Earth and Planetary Science Letters 307:59-70

Heaman LM, Kjarsgaard BA, Creaser RA (2003) The timing of kimberlite magmatism in North America: implications for global kimberlite genesis and diamond exploration. Lithos 71:153-184

Huntley DH, Little E, Duk-Rodkin A, Sandeman H (2006) Drift geochemistry of south-Central Mackenzie Valley watershed: New hypotheses resulting from Reconnaissance Drift and stream sediment sampling surveys in the NWT. 34th Annual Yellowknife Geoscience Forum poster

Huntley DH, Mills A, Paulen R (2008) Surficial deposits, landforms, glacial history, and reconnaissance drift sampling in the Trout Lake map area, Northwest Territories. Geological Survey of Canada, Current Research 2008-14, p. 14

Janse AJ (1994) Is Clifford's Rule still valid? Affirmative examples from around the world. In: Meyer HOA, Leonardos OH (eds) Diamonds: characterization, genesis and exploration. Proceedings, Fifth International Kimberlite Conference, vol 2, pp 215-235

Kerr DE, Kjarsgaard IM, Smith D (2000) Chemical characteristics of kimberlite indicator minerals from the Drybones Bay area (NTS 85I/4), Northwest Territories. Geological Survey of Canada, GSC Open File 3942

Le Maitre RW (1982) Multiple discriminant analysis. In: Le Maitre RW (eds.) Numerical petrology: statistical interpretation of geochemical data, Elsevier pp 141-158

Malkovets VG, Rezvukhin DI, Belousova EA, Griffin WL, Sharygin IS, Tretiakova IG, Gibsher AA, O'Reilly SY, Kuzmin DV, Litasov KD, Logvinova AM (2016) Cr-rich rutile: A powerful tool for diamond exploration. Lithos 265:304-311

Margold M, Stokes CR, Clark CD, Kleman J (2015) Ice streams in the Laurentide Ice Sheet: a new mapping inventory. Journal of Maps 11:380-395

Mather KA, Pearson DG, McKenzie D, Kjarsgaard BA, Priestley K (2011) Constraints on the depth and thermal history of Cratonic lithosphere from peridotite xenoliths, xenocrysts and seismology. Lithos 125:729-742

McClenaghan MB (2005) Indicator mineral methods in mineral exploration. Geochemistry: Exploration, Environment, Analysis 5:233-245

McClenaghan MB, Ward BC, Kjarsgaard IM, Kjarsgaard BA, Kerr DE, Dredge LA (2002) Indicator mineral and till geochemical dispersal patterns associated with the Ranch Lake kimberlite, Lac de Gras region, NWT, Canada. Geochemistry: Exploration, Environment, Analysis 2:299-319

McDonough WF, Sun SS (1995) The composition of the Earth. Chemical geology 120:223-253

Meijer Drees NC (1975) Geology of the Lower Paleozoic formations in the subsurface of the Fort Simpson area, District of Mackenzie, Northwest Territories, Geological Survey of Canada, Paper 74-40, p. 65

Meijer-Drees NC (1993) The Devonian succession in the subsurface of the Great Slave and Great Bear plains, Northwest Territories. Geological Survey of Canada

Menzies A, Westerlund K, Grütter H, Gurney J, Carlson J, Fung A, Nowicki T (2004) Peridotitic mantle xenoliths from kimberlites on the Ekati Diamond Mine property, NWT, Canada: major element compositions and implications for the lithosphere beneath the Central Slave craton. Lithos 77:395-412

Mills AJ (2008) Phase II Non-renewable Resource Assessment: analysis and interpretation of regional stream sediment and water results for Edéhzhíe Candidate Protected Area, Northwest Territories, Canada. NWT Geoscience Office Open File 2008-03

Morris TF, Sage RP, Ayer JA, Crabtree DC (2002) A study in clinopyroxene composition: implications for kimberlite exploration. Geochemistry: Exploration, environment, analysis 2:321-331

Nimis P (1998) Clinopyroxene geobarometry of pyroxenitic xenoliths from Hyblean Plateau (SE Sicily, Italy). European Journal of Mineralogy 22:521-534

Nimis P, Taylor WR (2000) Single clinopyroxene thermobarometry for garnet peridotites. Part I. Calibration and testing of a Cr-in-Cpx barometer and an enstatite-in-Cpx thermometer. Contributions to Mineralogy and Petrology 139:541-554

Nowell GM, Pearson DG, Bell DR, Carlson RW, Smith CB, Kempton PD, Noble SR (2004) Hf isotope systematics of kimberlites and their megacrysts: new constraints on their source regions. Journal of Petrology 45:1583-1612

Ootes L, Davis WJ, Jackson VA, van Breemen O (2015) Chronostratigraphy of the Hottah terrane and Great Bear magmatic zone of Wopmay orogen, Canada, and exploration of a terrane translation model. Canadian Journal of Earth Sciences, 12:1062-1092

Parent M, Paradis SJ, Doiron A (1996) Palimpsest glacial dispersal trains and their significance for drift prospecting. Journal of Geochemical Exploration 56:123-140

Paulen RC (2009) Sampling techniques in the Western Canada Sedimentary Basin and the Cordillera. In: Paulen RC, McMartin I (eds) Application of Till and Stream Sediment

Heavy Mineral and Geochemical Methods to Mineral Exploration in Western and Northern Canada, pp 49-74

Paulen RC (2013) A Revised look at Canada's landscape: Glacial processes and dynamics. In: Paulen RC, McClenaghan MB (eds.) New Frontiers for Exploration in Glaciated Terrain, pp 21-26

Pitman PW (2014) Technical report on the HOAM project, Northwest Territories, Canada NTS Map Sheets 85L, 85M, 95A, 95G, 95H, 95I, 95J, 95O, 95P, 96A and 96B. Olivut Resources Ltd. pp 1-55

Pohar M, Blas M, Turk S (2004) Comparison of logistic regression and linear discriminant analysis: a simulation study. Metodoloski zvezki 1:143-161

Pronk P (2008) Sambaa K'e Candidate Protected Area, Non-renewable Resource Assessment Phase I, Minerals. NWT Geoscience Office Open File Report 2008-08

Rampton VN (2000) Large-scale effects of subglacial meltwater flow in the southern Slave Province, Northwest Territories, Canada. Canadian Journal of Earth Sciences 37:81-93

Ramsay RR, Tompkins LA (1994) The geology, heavy mineral concentrate mineralogy, and diamond prospectivity of the Boa Esperança and Cana Verde pipes, Corrego D'anta, Minas Gerais, Brazil. Kimberlites, Related Rocks and Mantle Xenoliths 1:329-345

Reimann C, Filzmoser P (2000) Normal and lognormal data distribution in geochemistry: death of a myth. Consequences for the statistical treatment of geochemical and environmental data. Environmental geology 39:1001-1014

Roeder PL, Schulze DJ (2008) Crystallization of groundmass spinel in kimberlite. Journal of Petrology 49:1473-1495

Rutter NW, Hawes RJ, Catto NR (1993) Surficial geology, southern Mackenzie River valley, District of Mackenzie, Northwest Territories. GSC Map 1693A

Sarkar C, Heaman LM, Pearson DG (2015) Duration and periodicity of kimberlite volcanic activity in the Lac de Gras kimberlite field, Canada and some recommendations for kimberlite geochronology. Lithos 218:155-166

Schaeffer AJ, Lebedev S (2014) Imaging the North American continent using waveform inversion of global and USArray data. Earth and Planetary Science Letters 402:26-41

Schulze DJ (2003) A classification scheme for mantle-derived garnets in kimberlite: a tool for investigating the mantle and exploring for diamonds. Lithos 71:195-213

Schulze DJ, Anderson PF, Hearn Jr BC, Hetman CM (1995) Origin and significance of ilmenite megacrysts and macrocrysts from kimberlite. International Geology Review 37:780-812

Sobolev NV (1977) Deep-seated inclusions in kimberlites and the problem of the Upper Mantle composition. American Geophysical Union p. 259

Stachel T, Harris JW (2008) The origin of cratonic diamonds—constraints from mineral inclusions. Ore Geology Reviews 34:5-32

Stott DF, Caldwell WG, Cant DJ, Christopher JE, Dixon J, Koster EH, McNeil DH, Simpson F (1993) Cretaceous. In: Stott DR, Aitken JD (eds) Sedimentary Cover of the Craton in Canada, Geological Society of America, pp 358-438

Villeneuve ME, Thériault RJ, Ross GM (1991) U–Pb ages and Sm–Nd signature of two subsurface granites from the Fort Simpson magnetic high, northwest Canada. Canadian Journal of Earth Sciences, 28:1003–1008

Watson DM (2010) Sambaa K'e Candidate Protected Area Phase II Non-renewable Resource Assessment –Minerals, Northwest Territories, Parts of NTS 085D,095A,B,H. NWT Geoscience Office Open File 2010-08

Williams GK (1985) Proterozoic, Mackenzie Corridor. Geological Survey of Canada, GSC Open File 1273

Wyatt BA, Baumgartner M, Anckar E, Grütter H (2004) Compositional classification of “kimberlitic” and “non-kimberlitic” ilmenite. Lithos 77:819-840

Zack T, Stockli DF, Luvizotto GL, Barth MG, Belousova E, Wolfe MR, Hinton RW (2011) In situ U–Pb rutile dating by LA-ICP-MS: 208 Pb correction and prospects for geological applications. Contributions to Mineralogy and Petrology 162:515-530

Figure captions:

Fig. 1 Bedrock geology map of Northwest Territories showing the Central Mackenzie Valley (CMV) sample locations for both study areas. Horn Plateau = Horn Plateau study area, Trout Lake = Trout Lake study area. Diamonds = kimberlites, dashed red line ellipse = outline Bulmer Lake gravity high. Black line = line of lithosphere seismic tomography cross-section (on bottom) from Schaefer and Lebedev (2014). See legend for rest of symbology and Fig. S1 for more detailed bedrock geology map. The prominent Horn Plateau in the centre of Horn Plateau (it rises 300-450 m above the surrounding plains) broadly correlates to the Late Cretaceous sedimentary rock outline (green; see cross-section below). Kimberlite locations after Pitman (2014) and NTGS GoData Kimberlite Anomaly and Drillhole Data (KANDD). Note pink indicates cold lithosphere for cross-section which is ~ 200 km thick lithosphere presently under most of CMV and Slave Craton

Fig. 2 Surficial geology map of Northwest Territories showing the Central Mackenzie Valley (CMV) sample locations for both study areas. Horn Plateau = Horn Plateau study area, Trout Lake = Trout Lake study area. Diamonds = kimberlites. See legend for the rest of symbology and Fig. S2 for more detailed surficial geology map. Surficial deposits and glacial flowlines after Fulton (1995)

Fig. 3 Clinopyroxene Cr_2O_3-Al_2O_3 discrimination plot (fields after Ramsey and Tompkins 1994). Grains from both study areas and 95 % contour interval fields for clinopyroxene from Central and Western Slave Craton surficial samples (grey dashed lines; data from NTGS GoData KIMC database). See legend for symbols. Note peridotitic grains have mg# > 0.88

Fig. 4 Garnet Cr_2O_3-CaO classification plot (after Grütter et al. 2004). Grains from both study areas and 95 % contour interval field for peridotitic garnets from CMV mineral claims (purple and yellow dashed lines; data from Pitman 2014), Central and Western Slave

Craton kimberlites (black dashed lines; data from variety of sources – see text) and surficial samples (grey dashed lines; data from NTGS GoData KIMC database). Solid red line = graphite diamond constraint (GDC). Double dashed green line = P_{38} Cr-in-garnet barometer (both after Grütter et al. 2006). Note P_{38} estimates 5.8 GPa (minimum) maximum pressure for Cr-rich garnets from the Horn Plateau

Fig. 5 Chondrite-normalized rare earth element (REE_N) plots for Horn Plateau peridotitic garnets. Chondrite normalization values after McDonough and Sun (1995). The garnets display three distinct REE_N patterns: HREE-enriched, an extreme sinusoidal MREE-depleted pattern and sinusoidal with variable re-enrichment. Mean values for n < 10, median values for n > 10. Symbol groupings are based on garnet classification after Grütter et al. (2004). Green triangles = G9, Blue squares = G10, Pink diamonds = G10D, Red circles = G11 and Purple crosses = G12 grains

Fig. 6 Ilmenite TiO_2-MgO discrimination plot (after Wyatt et al. 2004). Grains from both study areas and 95 % contour interval fields for Mg-ilmenites from Central and Western Slave Craton surficial samples (grey dashed lines; data from NTGS GoData KIMC database), as well as the Drybones Bay kimberlite (black dashed lines; data from Schulze et al. 1995; Kerr et al. 2000). See legend for symbology

Fig. 7 FITPLOT geotherms (following methodology of Mather et al. 2011) and clinopyroxene P–T data for both study areas and Central Slave Craton (data from Hasterok and Chapman 2011) using Nimis and Taylor (2000) thermobarometry technique. See legend for symbols. LDG = Lac de Gras, Solid red line = graphite diamond transition curve (after Day 2012), Solid black line = mantle adiabat with mantle potential temperature of 1350 °C. Upper and lower crust thicknesses for Horn Plateau was constrained from the SNORCLE line 1 transect (Cook et al. 1999). Depth was determined by multiplying pressure (GPa) by 3.15. Note the similarity between Central Slave Craton and Horn Plateau Cr-diopside geotherms

Fig. 8 Mantle sampling profiles of garnet peridotite minerals from the Horn Plateau samples. Left = single grain clinopyroxene barometer results (after Nimis and Taylor 2000). Centre = projected Ni-in-garnet temperatures (averages of Griffin et al. 1989 and Canil 1999). Right = projected Al-in-olivine temperatures (after Bussweiler et al. 2017). Red line = graphite-diamond transition curve (after Day 2012)

Fig. 9 Top – $^{176}Hf/^{177}Hf$ corrected ratios plot for MC-ICP-MS analyzed CMV kimberlitic (Mg-)ilmenites. Outlined in respective coloured boxes are the two age groups discussed in text: Yellow = Neoproterozoic-Silurian age group, Green = Devonian-Paleogene age group. Error bars signify internal standard error (2σ). **Bottom –** $^{176}Hf/^{177}Hf$ corrected mean ratios for ilmenites from North American Craton kimberlites, as well as those from the Udachnaya East kimberlite and Malaita alnöitic breccia. Error bars signify standard deviation at 95 % confidence interval (2σ). Coloured boxes represent the Horn Plateau age groups. See Table S4 for kimberlite localities, geochronology techniques used and sources of data

Fig. 10 Probability density plots for garnets, X-axis values assigned by logistic regression-solutions for peridotitic garnet major element data between Horn Plateau grains and those from various populations (see text for details). Increasing degrees of overlap indicate increasing difficulty in reconciling population, while offset distributions indicate population differences (see text for details)

Figure 1

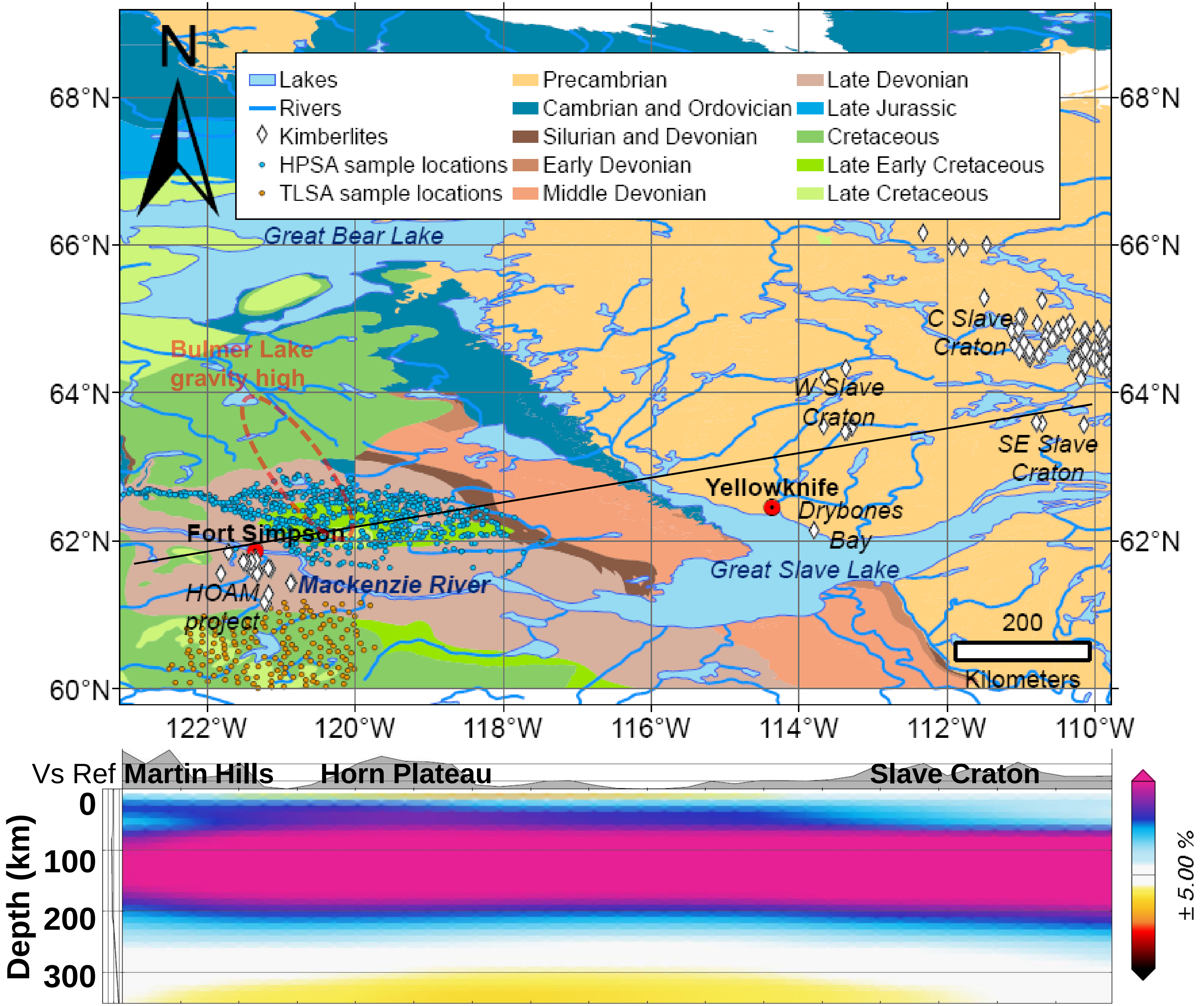

Lakes
Rivers
Kimberlites
HPSA sample locations
TLSA sample locations
Precambrian
Cambrian and Ordovician
Silurian and Devonian
Early Devonian
Middle Devonian
Late Devonian
Late Jurassic
Cretaceous
Late Early Cretaceous
Late Cretaceous
N
Great Bear Lake
Bulmer Lake gravity high
C Slave Craton
W Slave Craton
SE Slave Craton
Yellowknife
Drybones Bay
Fort Simpson
Great Slave Lake
Mackenzie River
HOAM project
200
Kilometers
122°W
120°W
118°W
116°W
114°W
112°W
110°W
68°N
66°N
64°N
62°N
60°N
Vs Ref
Martin Hills
Horn Plateau
Slave Craton
Depth (km)
0
100
200
300
± 5.00 %

Figure 2

Click here to download Colour Figure Poitras et al._IKC-Figure2.pptx

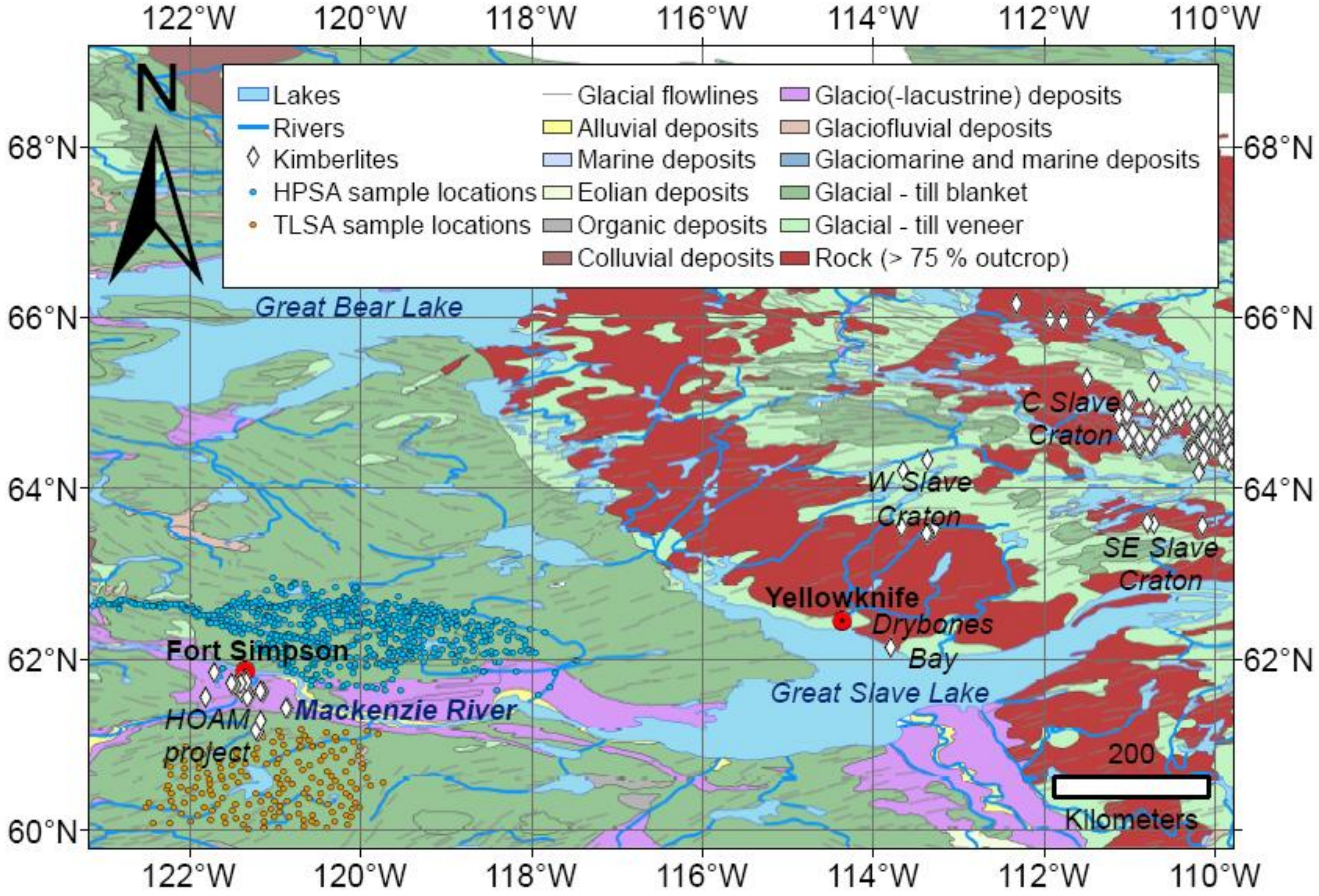

Figure 3

Click here to download Colour Figure Poitras et al._IKC-Figure3.pptx

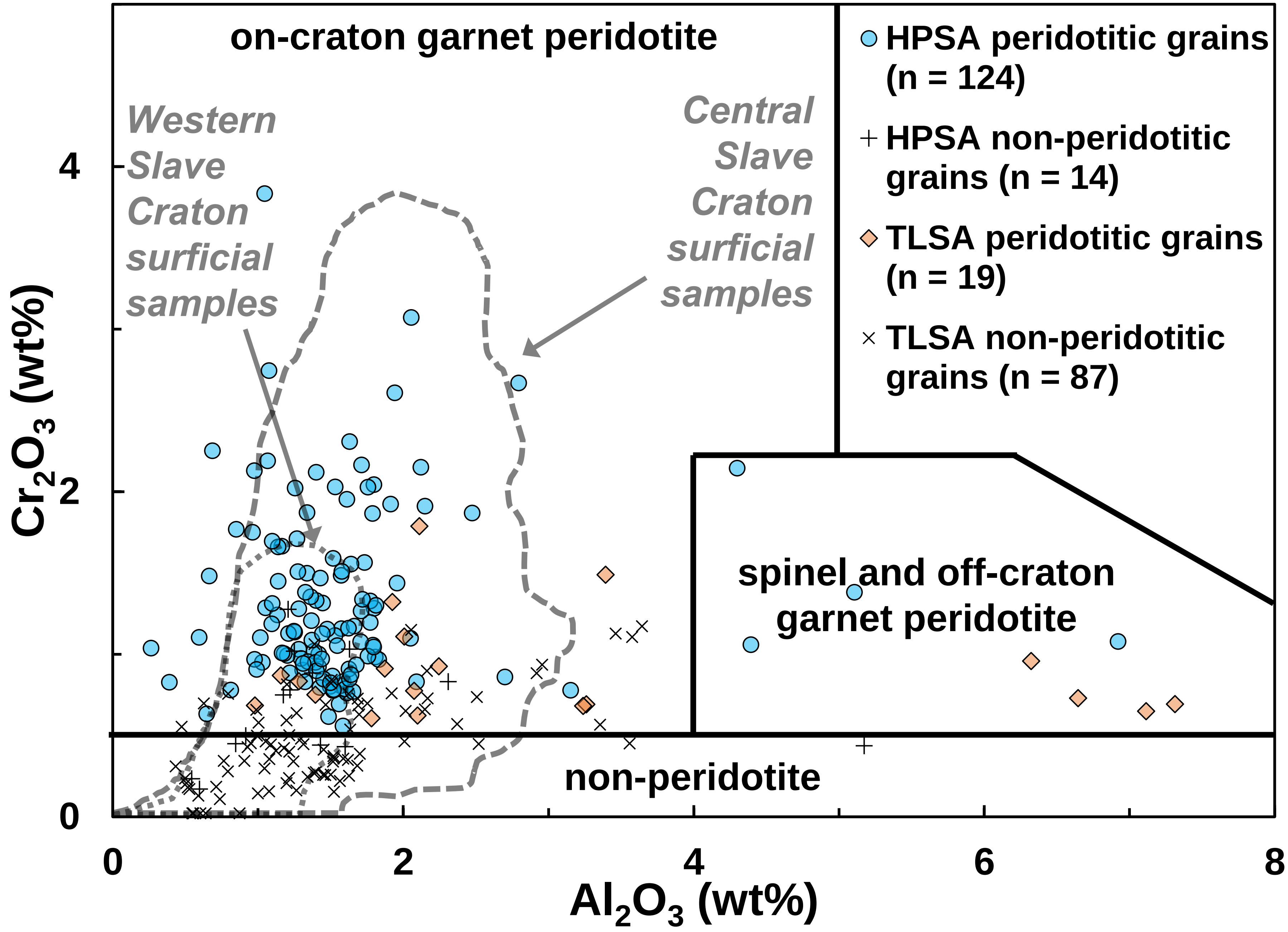

Figure 4

Click here to download Colour Figure Poitras et al._IKC-Figure4.pptx

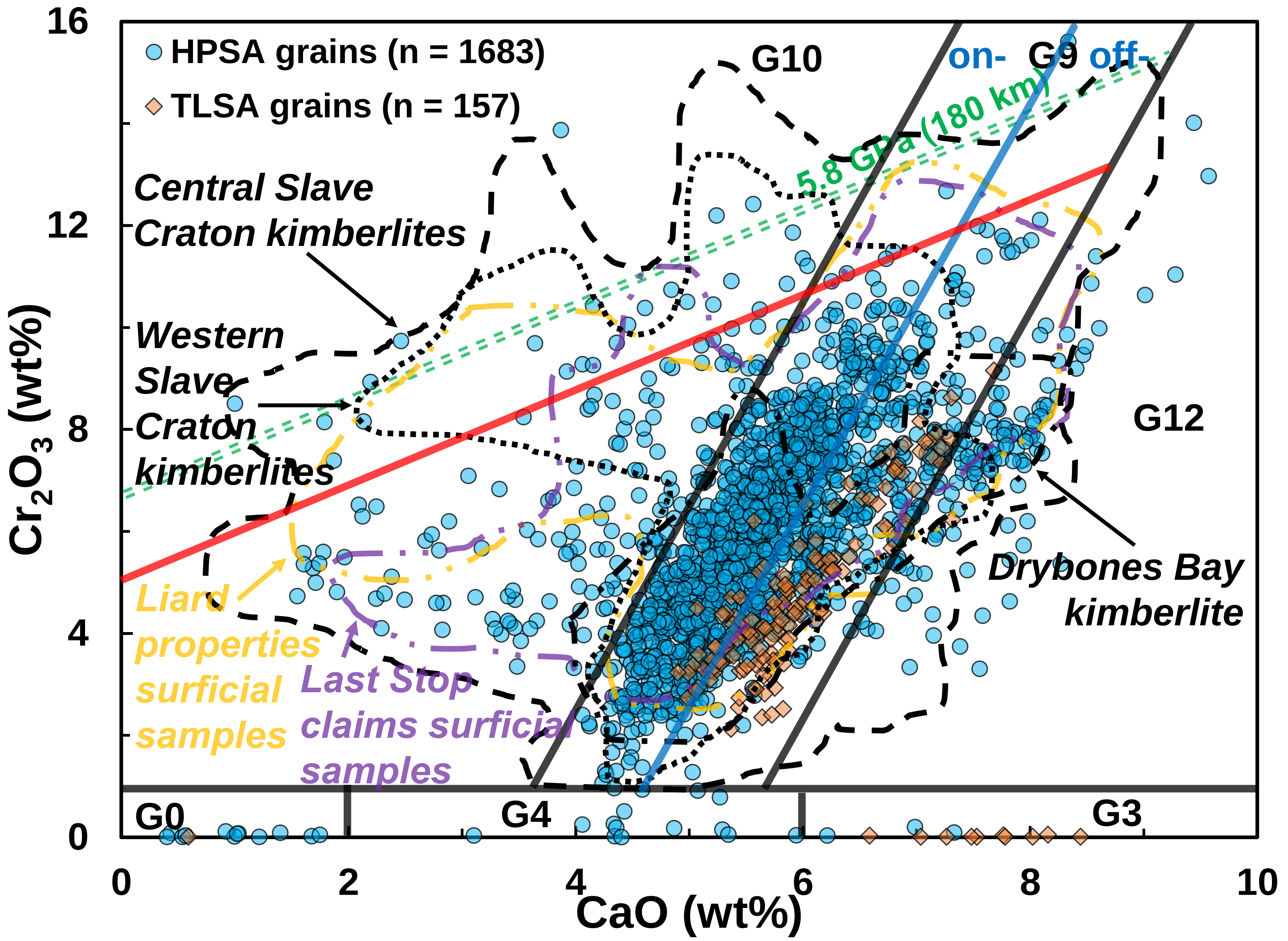

Figure 5

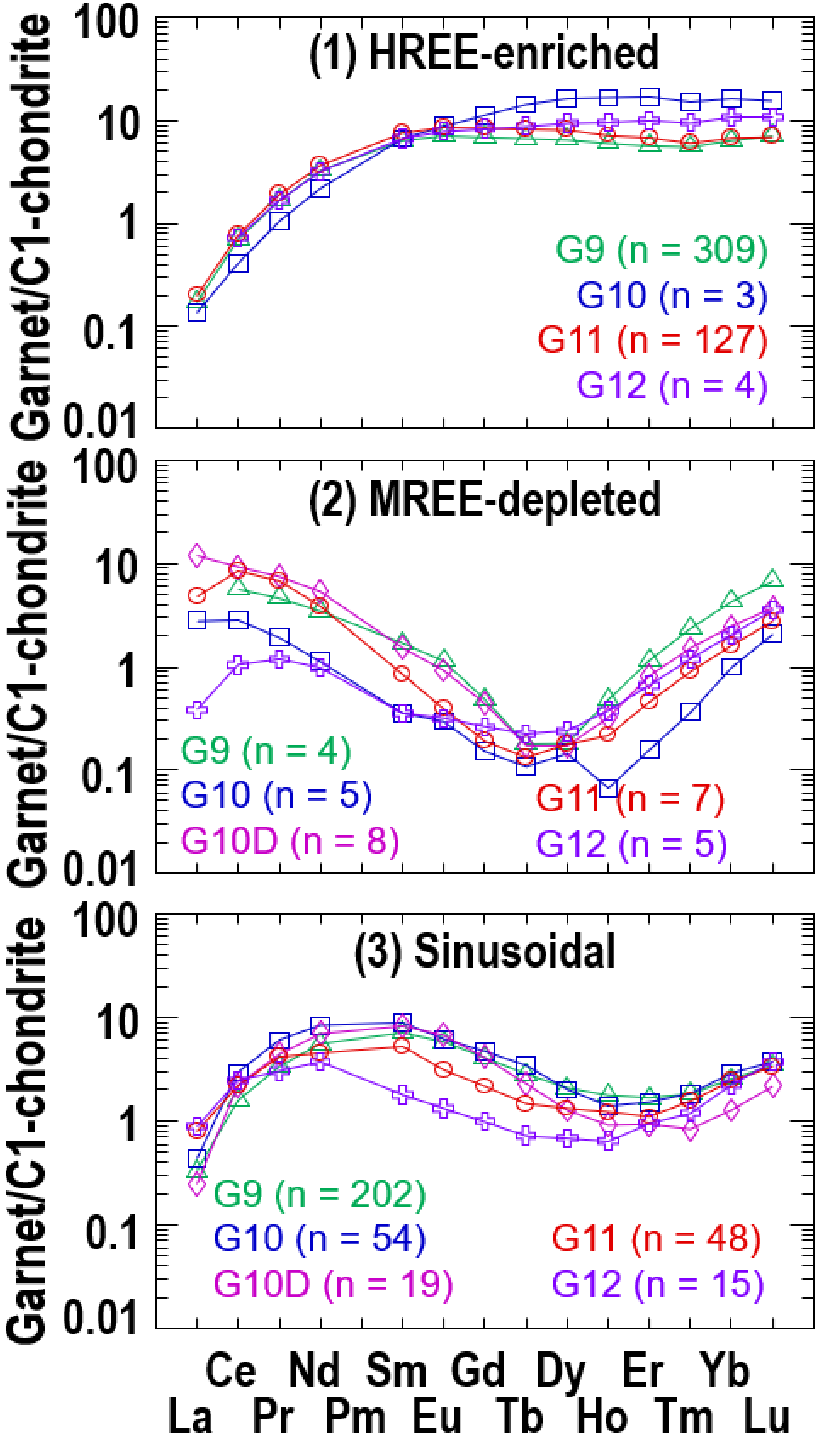

(1) HREE-enriched
G9 (n = 309)
G10 (n = 3)
G11 (n = 127)
G12 (n = 4)
(2) MREE-depleted
G9 (n = 4)
G10 (n = 5)
G10D (n = 8)
G11 (n = 7)
G12 (n = 5)
(3) Sinusoidal
G9 (n = 202)
G10 (n = 54)
G10D (n = 19)
G11 (n = 48)
G12 (n = 15)
Garnet/C1-chondrite
100
10
1
0.1
0.01
La Ce Pr Nd Pm Sm Eu Gd Tb Dy Ho Er Tm Yb Lu

Figure 6

Click here to download Colour Figure Poitras et al._IKC-Figure6.pptx

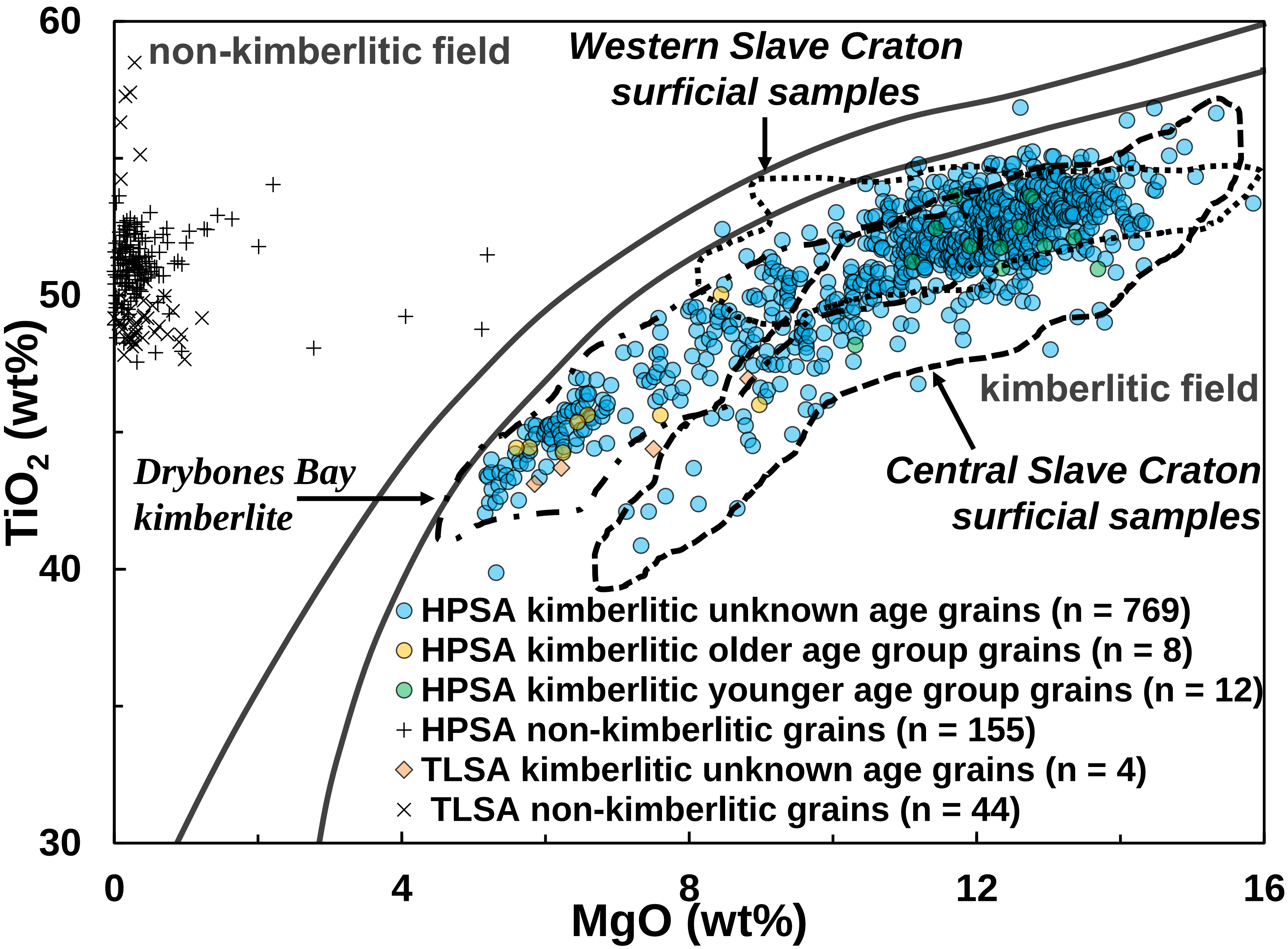

Figure 7

Click here to download Colour Figure Poitras et al._IKC-Figure7.pptx

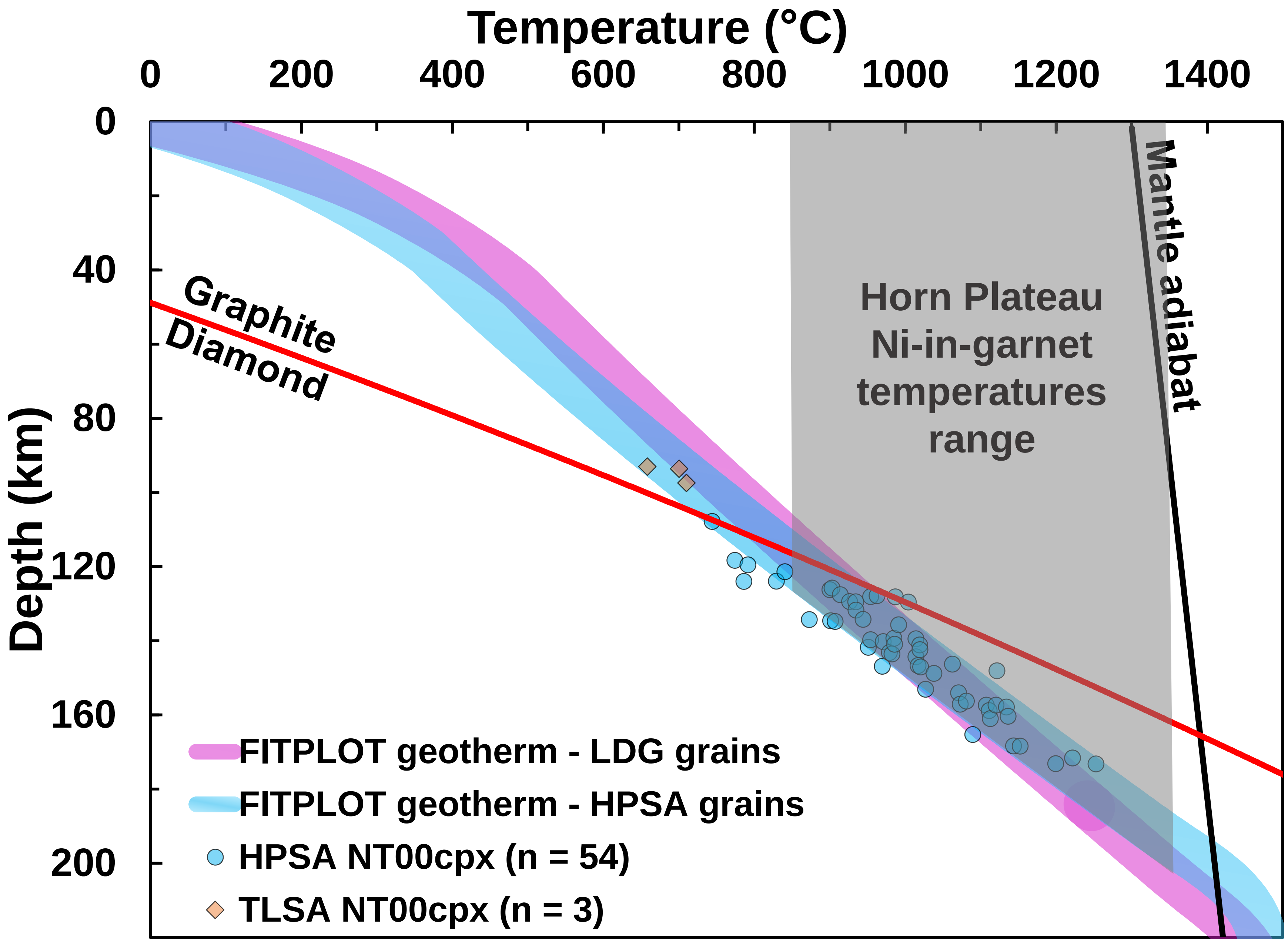

Figure 8

Click here to download Colour Figure Poitras et al._IKC-Figure8.pptx

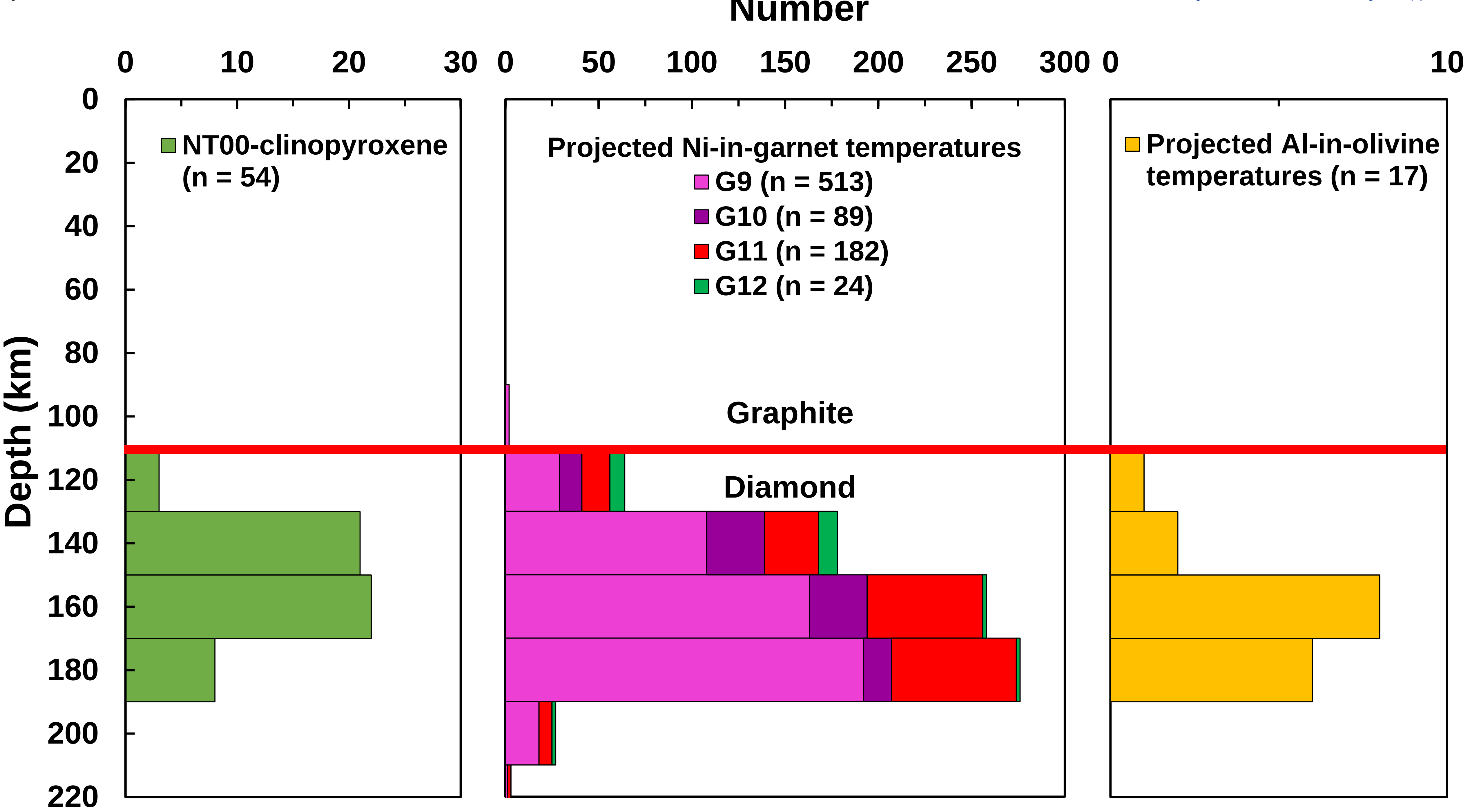

Figure 9

Click here to download Colour Figure Poitras et al._IKC-Figure9.pptx

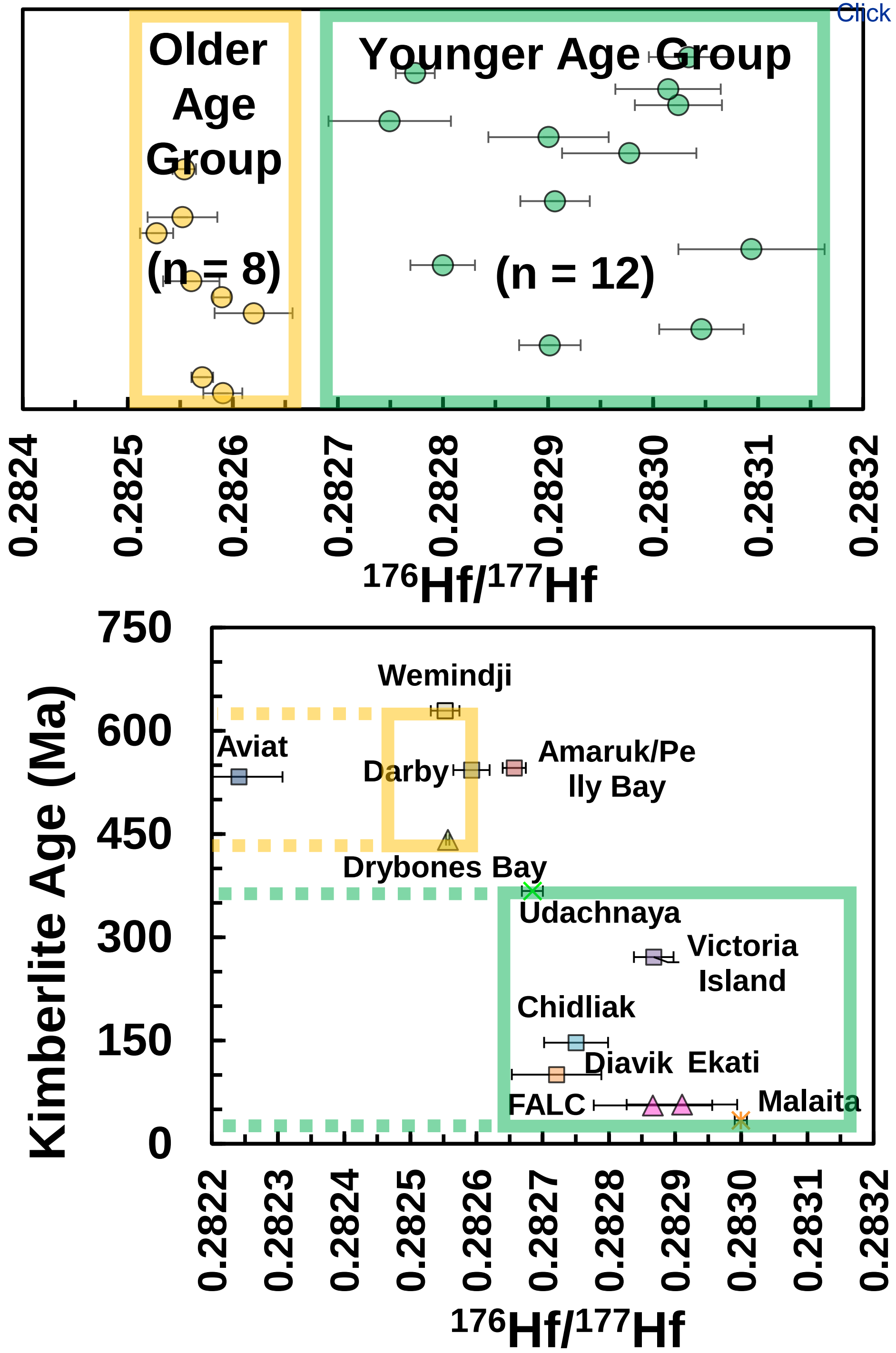

Figure 10

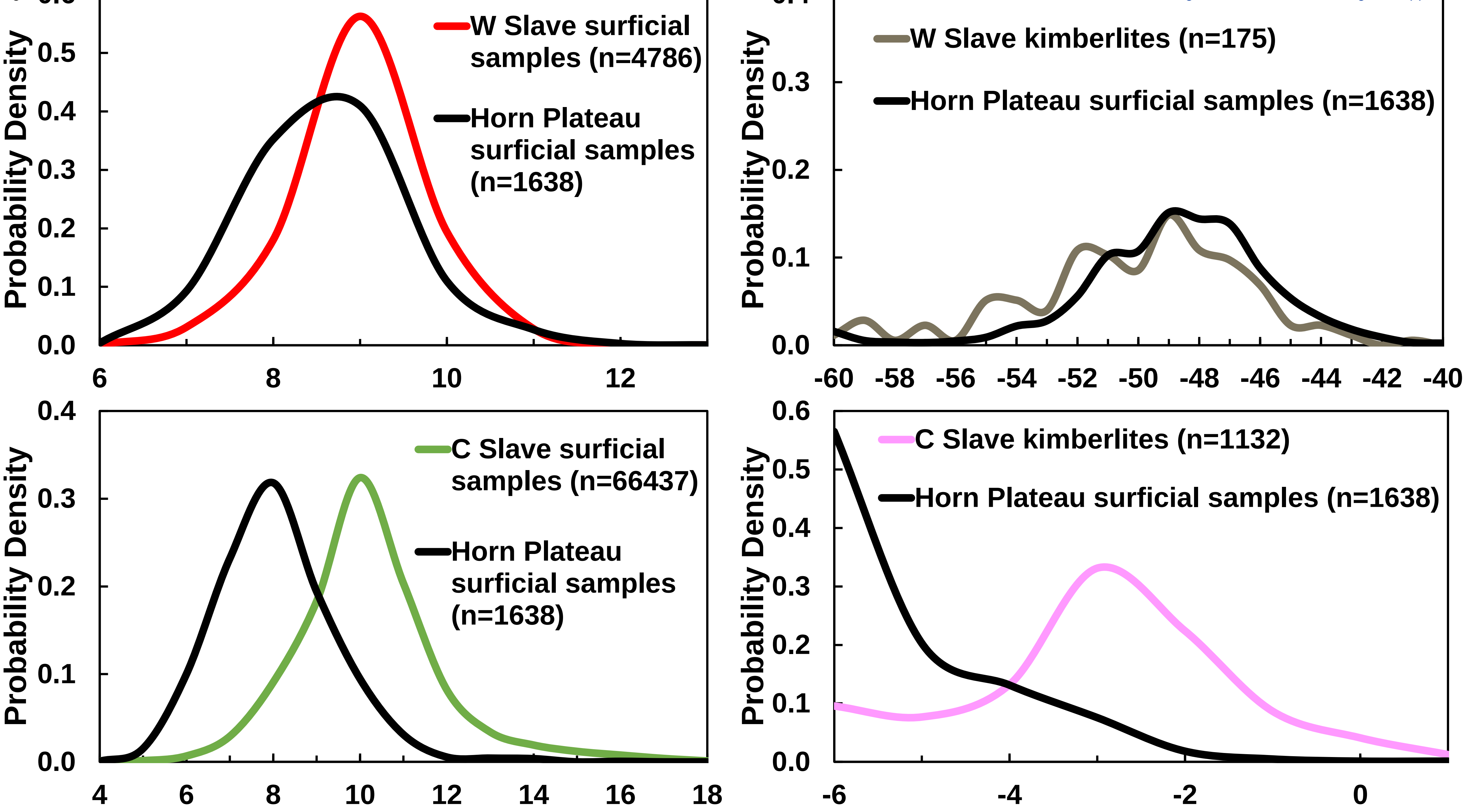
W Slave surficial samples (n=4786)
Horn Plateau surficial samples (n=1638)
Probability Density
0.0
0.1
0.2
0.3
0.4
0.5
0.6
6
8
10
12
W Slave kimberlites (n=175)
Horn Plateau surficial samples (n=1638)
Probability Density
0.0
0.1
0.2
0.3
0.4
-60
-58
-56
-54
-52
-50
-48
-46
-44
-42
-40
C Slave surficial samples (n=66437)
Horn Plateau surficial samples (n=1638)
Probability Density
0.0
0.1
0.2
0.3
0.4
4
6
8
10
12
14
16
18
C Slave kimberlites (n=1132)
Horn Plateau surficial samples (n=1638)
Probability Density
0.0
0.1
0.2
0.3
0.4
0.5
0.6
-6
-4
-2
0